JAEA-Data/Code
2019-017
DOI:10.11484/jaea-data-code-2019-017

JAEA-Data/Code

Fission Product Chemistry Database ECUME Version 1.1

Development Group for LWR Advanced Technology

LWR Key Technology Development Division
Nuclear Science and Engineering Center
Nuclear Science Research Institute
Sector of Nuclear Science Research

March 2020

Japan Atomic Energy Agency

日本原子力研究開発機構

本レポートは国立研究開発法人日本原子力研究開発機構が不定期に発行する成果報告書です。
本レポートの入手並びに著作権利用に関するお問い合わせは、下記あてにお問い合わせ下さい。
なお、本レポートの全文は日本原子力研究開発機構ホームページ（https://www.jaea.go.jp）
より発信されています。

国立研究開発法人日本原子力研究開発機構 研究連携成果展開部 研究成果管理課
〒319-1195 茨城県那珂郡東海村大字白方 2 番地4
電話 029-282-6387, Fax 029-282-5920, E-mail:ird-support@jaea.go.jp

This report is issued irregularly by Japan Atomic Energy Agency.
Inquiries about availability and/or copyright of this report should be addressed to
Institutional Repository Section,
Intellectual Resources Management and R&D Collaboration Department,
Japan Atomic Energy Agency.
2-4 Shirakata, Tokai-mura, Naka-gun, Ibaraki-ken 319-1195 Japan
Tel +81-29-282-6387, Fax +81-29-282-5920, E-mail:ird-support@jaea.go.jp

JAEA-Data/Code 2019-017

Fission Product Chemistry Database ECUME Version 1.1

Development Group for LWR Advanced Technology

LWR Key Technology Development Division, Nuclear Science and Engineering Center,
Nuclear Science Research Institute, Sector of Nuclear Science Research,
Japan Atomic Energy Agency
Tokai-mura, Naka-gun, Ibaraki-ken

(Received November 22, 2019)

This technical report presents an extended first version (version 1.1) of the fission product (FP) chemistry database, which is named Effective Chemistry database of fission products Under Multiphase rEaction (ECUME). ECUME is the database that is used for the analyses of FP chemistry, which considerably affects all FP behaviors during severe accidents (SAs) at nuclear facilities such as LWR. ECUME consists of three types of datasets: dataset for Chemical Reaction Kinetics (CRK), Elemental Model set (EM), and ThermoDynamic dataset (TD). This version of ECUME is prepared to more accurately evaluate Cs and I distribution in the reactor and release amount into the environment, which is essential for the decommissioning of Fukushima Daiichi Nuclear Power Station of Tokyo Electric Power Company Holdings, Inc. (1F) and the enhancement of LWR safety after the 1F SA. Thus, this version of ECUME is mainly equipped with the datasets for Cs and I chemistry: CRK for the reaction of Cs-I-B-Mo-O-H and Ru-N-O-H systems in gas phase, EM for the Cs chemical reaction with stainless steel (SS) (Cs chemisorption onto SS), and TD for $CsBO_2$ vapor species and solid $Cs_2Si_4O_9$ and $CsFeSiO_4$.

CRKs were prepared either by referring to previous studies or calculation results using a combinational method of *ab-initio* calculation with statistical physics (if the literature data were not available such as for the reactions between Cs and B/Mo, oxidation of Ru). EM was prepared by analyzing the experimental results and reproducing Cs chemisorption onto SS under various chemical conditions. TDs for $CsBO_2$ vapor species and solid $Cs_2Si_4O_9$ were prepared based on the vapor pressure measurement results and heat capacity measurement results, respectively. TD for solid $CsFeSiO_4$ with no available experimental data was prepared using *ab-initio*-based methodology that was developed for this purpose.

This version of ECUME was successfully verified. The effects of B vapor and Fe, Si in SS on Cs behavior can be evaluated by improving current SA analysis codes using ECUME, which will result in a more accurate evaluation of Cs distribution at 1F and release amount into the environment. Thus, ECUME provides the fundamental solution for the FP chemistry issues for the 1F decommissioning work and enhancement of LWR safety after the 1F SA.

Keywords: Fission Product, Chemistry, Cesium, Iodine, Severe Accident, Database, ECUME

JAEA-Data/Code 2019-017

核分裂生成物化学挙動データベース ECUME Version 1.1

日本原子力研究開発機構　原子力科学研究部門　原子力科学研究所
原子力基礎工学研究センター　軽水炉基盤技術開発ディビジョン

性能高度化技術開発グループ

（2019 年 11 月 22 日受理）

本技術報告書は、核分裂生成物（FP）化学挙動データベース ECUME（Effective Chemistry database of fission products Under Multiphase rEaction）の初版（拡張版：version 1.1）を示す。ECUME は、軽水炉等の原子力施設の重大事故時の FP 挙動を支配する化学挙動を評価するために必要な化学反応速度定数データセット CRK（dataset for Chemical Reaction Kinetics）、要素モデルセット EM (Elemental Model set)、そして熱力学データセット TD（ThermoDynamic dataset）の 3 つのデータセットから構成されている。ECUME 初版（拡張版）は、特に東京電力ホールディングス株式会社福島第一原子力発電所（1F）の廃炉やそれを受けた軽水炉の安全性向上の取り組みにおいて重要なセシウム（Cs）、ヨウ素（I）を主な対象として、これらの炉内分布や環境放出量をより正確に評価できるように整備した。したがって、ECUME 初版（拡張版）には、Cs-I-B-Mo-O-H 系及び Ru-N-O-H 系の気相反応の CRK、鋼材への Cs の化学反応（鋼材への Cs 化学吸着）を対象とした EM、そして $CsBO_2$ 蒸気、固体 $Cs_2Si_4O_9$、固体 $CsFeSiO_4$ の各化合物の TD を格納している。

CRK は、既往の化学反応速度定数データを文献から収集するとともに、データの無い Cs と B/Mo の反応や Ru の酸化反応については、統計物理学を適用した第一原理計算によりデータを取得して整備した。EM は、多様な化学条件における Cs 化学吸着実験を実施し、取得したデータを解析することにより整備した。TD で $CsBO_2$ や $Cs_2Si_4O_9$ は、それぞれ蒸気圧測定や比熱測定により実験データを取得し、実験データが無い $CsFeSiO_4$ は、このために開発した第一原理計算を用いてデータを整備した。

ECUME は、重大事故時におけるより正確な FP 挙動評価への貢献が期待できる。ECUME を用いて既往の SA 解析コードを改良することにより、Cs 挙動に与える B 蒸気の影響や鋼材中の Fe や Si の影響を評価することが可能となり、1F 炉内の Cs 分布や環境放出量をより正確に評価できるようになる。このように、ECUME は、1F 廃炉や軽水炉の安全性向上に向けた取り組みにおける FP 化学挙動に関する課題に対して根本的な解決方法を提供するものである。

原子力科学研究所：〒319-1195 茨城県那珂郡東海村大字白方 2 番地 4

Contents

目次

Table list

Figure list

表リスト

図リスト

Nomenclature

A: Pre-exponential factor ($cm^3/mol/K^n/s$)

B_e: Rotational constant for diatomic molecules (1/cm)

c_2: Second radiation constant (cm･K)

C_l: Dissolved Cs concentration in the Noyes-Whitney equation (mol/m^3)

C_g: Concentration of CsOH in the gas phase (μg $CsOH/cm^3$)

C_p: Heat capacity at constant pressure (J/mol/K)

C_S: Cs concentration of saturated solution in the Noyes-Whitney equation (mol/m^3)

C_w: Concentration of the gas species at the surface of solid (mol/m^3)

C_∞: Concentration of the bulk gas species (mol/m^3)

d_p: Diameter of particle (m)

d_{dr}: Diameter of droplet (m)

D_S: Diffusion coefficient of Cs reactant species in solid phase (cm^2/s)

E: Activation energy (J/mol)

g_i: quantum (or statistical) weight of the i-th electronic state

$-(G°-H_{298}°)/T$: Gibbs energy function (J/mol/K)

h: Planck's constant (J･s)

H: Enthalpy (J/mol)

H_S: Solubility coefficient (-)

I: Moment of inertia ($g･cm^2$)

k'': Second-order reaction rate constant (1/s/wt.%)

k_f: Forward chemical reaction rate constant (1/s)

k_r: Reverse chemical reaction rate constant (1/s)

k_a: Dissolution rate constant in the Noyes-Whitney equation ($1/m^2/s$)

k_B: Boltzmann constant (J/K)

k_g: Gas mass transfer coefficient for the gas species (m/s)

K_{eq}: Equilibrium constant (-)

m: Molecular mass (kg)

n: Real number

N: Chemisorption amount per unit time unit area in the Bowsher's model (μg $Cs/cm^2/s$)

N_w: Transported gas amount from gas phase to the surface of solid per unit time unit area in the mass transfer model ($mol/m^2/s$)

p: Equilibrium vapor pressure (Pa)

Q_e: Electronic partition function (-)

Q_r: Rotational partition function (-)

Q_t: Translational partition function (-)

Q_v: Vibrational partition function (-)

R: Gas constant (J/mol/K)

S: Entropy (J/mol/K)

S_p: Surface area of exposed solid in the Noyes-Whitney equation (m^2)

t: Time (s)

T: Absolute temperature (K)

u: $u = c_2(\omega_e - 2\omega_e\chi_e)/T$ for an anharmonic oscillation model, $u = c_2\omega/T$ for a harmonic oscillator

V: Gas volume (m^3)

v_d: Surface reaction rate constant in the Bowsher's model (cm/s)

v_{dri}: Velocity of initial droplet (m/s)

v_p: Velocity of particle (m/s)

α_e: First-order rotation-vibration interaction constant (1/cm)

β: $\beta = 8\pi^2 I k_B T/\sigma h^2$ for rigid rotor model, $\beta = T/(B_e - \alpha_e/2)/c_2$ for a non-rigid rotor model

δ: Random number

ε: Electron energy level

υ: Vibrational frequency (1/s)

θ: Fraction of reaction site on the deposit surface

η: Removal efficiency of a single droplet in the aerosol removal model
(impaction of single droplet efficiency)

ψ: Stokes number (-)

ρ_p: Density of particle (kg/m^3)

μ_g: Viscosity of gas (kg/m/s)

σ: Symmetry number of molecules

ω: Fundamental vibrational frequency of a harmonic oscillator (1/cm)

ω_e: Vibrational fundamental for infinitesimal amplitude (1/cm)

$\omega_e\chi_e$: Vibrational anharmonicity constant (1/cm)

(Superscripts)

i: i-th state

°: Standard state pressure of 1 bar (0.1 MPa)

(Subscripts)

f: Formation

i: i-th state

TS: Transition State

tr: Phase transition

1. Introduction

1.1. Issues for source term evaluation

The improvement of source term under LWR severe accidents (SAs) is essential both for the continuous enhancement of LWR safety[1,2,3,4] and the decommissioning of Fukushima Daiichi Nuclear Power Station of Tokyo Electric Power Company Holdings, Inc. (1F)[5]. The main tool used to evaluate the source term has been and will be the SA analysis codes such as MELCOR[6], MAAP[7], SAMPSON[8], THALES-2[9]. The SA analysis codes can estimate the release of fission products (FPs) into the environment and the distribution of FPs in the reactor based on the models of thermal-hydraulics and FP behaviors at each region in the reactor, from reactor pressure vessel (RPV) to containment vessel (CV) and reactor building (RB) through reactor cooling system. Thus, the improvement of FP models is essential for the improved source term[10]. The FP models have been improved based on the results from studies on various FP behaviors[11,12,13].

FP chemistry has been recognized as the most effective and promising way for the overall improvement of source term[2,14] because the FP chemistry considerably affects the FP release and transport behavior. Therefore, various studies on FP chemistry aiming at improving FP models have been conducted since the TMI-2 SA and are still in progress[15,16]. The key point for the FP chemistry research is to prepare a comprehensive but rational FP chemistry database that covers all important chemical features of possible LWR SA sequences. The FP chemical models can be constructed to describe a representative chemical condition at SAs based on such comprehensive and rational FP chemistry database. However, until now, such database has not been available.

1.2. FP chemistry research in JAEA

In response to the abovementioned FP chemistry issues, we conducting a fundamental study on the FP chemistry to construct a comprehensive and rational FP chemistry database[16,17]. The role of database in the framework of our FP chemistry study is shown in Figure 1. Our FP chemistry database is named Effective Chemistry database of fission products Under Multiphase rEaction (ECUME)[18]. The outputs based on ECUME are not only FP chemical models that can be implemented for SA analysis codes but also basic knowledge and data obtained through chemical analyses with ECUME using a 3D-CFD analysis code with a fine space resolution[19]. These outputs will improve the source term for both the enhancement of LWR safety after the 1F SA and the 1F decommissioning work. This study covers important chemistry-related phenomena that were revealed after the 1F SA such as the chemical effects of boron (B)[20,21], chemical interaction between FP vapor/aerosol and structural materials[22,23], and the effect of solubility of FP deposited compounds on the leaching behavior. The aerosol behavior is also included because it is affected by the chemical properties such as condensation and hygroscopic properties.

In this technical report, the extended first version (version 1.1) of ECUME[18] is presented. ECUME provides useful datasets and models for the commercially/freely available calculation tools, such as the SA analysis codes, to more accurately estimate the FP chemistry.

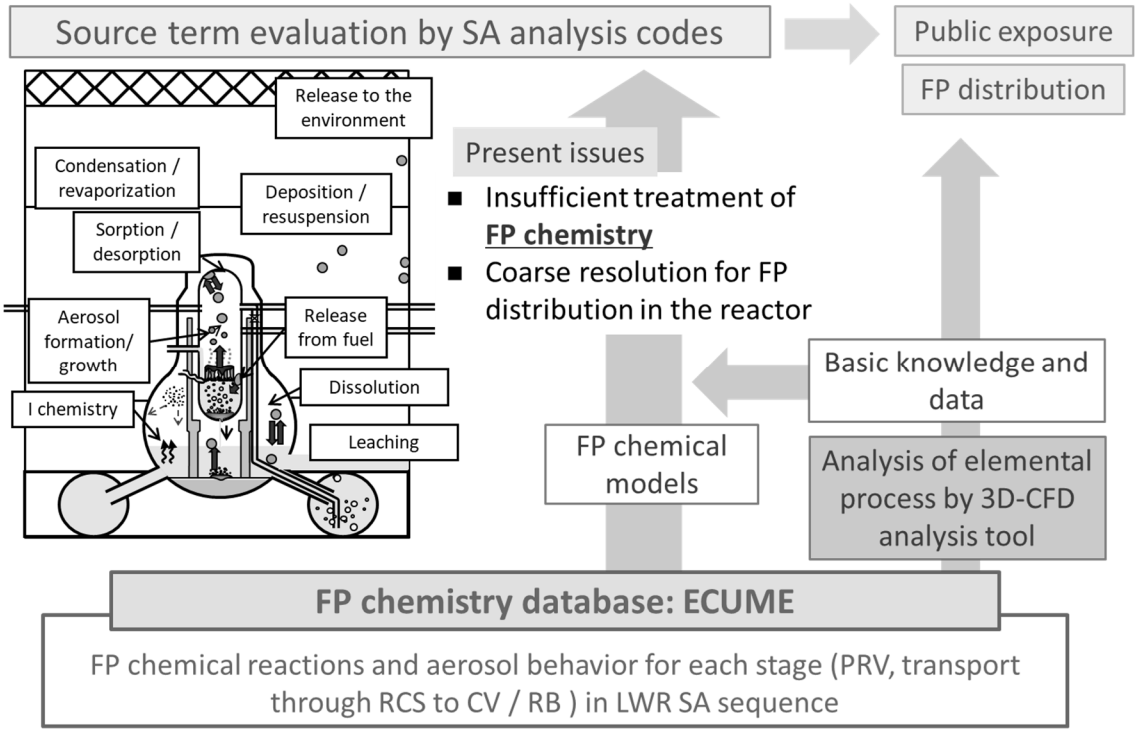

Figure 1 Role of ECUME in the framework of our FP chemistry study

2. FP chemistry database ECUME

ECUME consists of three types of datasets: dataset for Chemical Reaction Kinetics (CRK), Elemental Model set (EM), and ThermoDynamic dataset (TD). Table 1 shows the contents of ECUME that are expected in the final version. The focal phenomena and behaviors were chosen on the basis of importance and priority in terms of both the 1F decommissioning work and the enhancement of LWR safety after the 1F SA.

2.1. Chemical system

The cesium (Cs) and iodine (I) are the most important FPs because large amounts of Cs and I are released into environment during an SA, which considerably affects the public exposure. Specifically, Cs is important for the evaluation of dose distribution at 1F[5)]. Thus, the main datasets and models are for the chemical system of Cs (i.e., Cs-137) and I (i.e., I-131). Since the BWR control and FP materials, boron (B) and molybdenum (Mo) respectively, have high chemical affinities and, thus, affects the chemistry of Cs and I, they are also included[14,20)]. In addition, because iron (Fe and silicon (Si) can form compounds with Cs during the chemical reaction between Cs and stainless steel (SS) (hereafter, Cs chemisorption onto SS)[22,23)], they are also considered.

In addition, because Ruthenium (Ru) has a potentially high radiological impact, it is also included in ECUME. Ru release can be considerably enhanced during the air-ingress scenario of PWR-SA and reprocessing plant accident[24)]. Strontium (Sr) chemistry will be also included because considerable amounts of Sr were released to the outside of the 1F RB through the aqueous phase[25)]. In addition, there is possibility that Sr release is enhanced during a likely chemical condition at 1F such as the co-existence of chlorine (Cl) by sea water injection[26)].

Consequently, the chemical systems of Cs-I-Mo-B-Fe-Si-O-H, Ru-N-O-H, and Sr-Cl-O are treated in ECUME.

2.2. Phenomena and behaviors

The phenomena and behaviors described in ECUME are not only chemical reactions in the gas phase but also those in the solid–gas phase. The main targets for the solid–gas phase reaction are the chemical interactions of B with deposits of Cs and I, and Cs chemisorption onto SS and re-vaporization. The chemical interaction of B with the deposits of Cs and I may cause a re-vaporization of gaseous iodine and Cs vapor species (hereafter, B-driven Cs and I re-vaporization)[27)]. This interaction is important in terms of a late phase environmental release. Cs chemisorption and re-vaporization affect Cs chemical speciation during transportation and Cs distribution in the RPV at 1F[22,23)]. This is an important behavior for the decommissioning and debris removal work at 1F.

The FP aerosol behavior will be also included in the future version of ECUME. The aerosol behavior in RB (specifically the interaction of aerosol with water droplets and resuspension behavior) were considered to be important for the reduction of uncertainty in the evaluation of source term. Models for these behaviors in this SA analysis code should be improved.

The long-term FP migration behavior through the aqueous phase becomes important for the 1F decommissioning work. The migration of dissolved FPs from fuel debris or deposit compounds onto structure materials (e.g., concrete and SS) to the aqueous phase may cause the secondary contamination for many years after an SA. This migration and contamination affect the debris removal and waste disposal work at 1F.

2.3. Dataset and model

Each dataset/model set in ECUME was designed to be directly or easily implemented in the current SA analysis code and numerical analysis tools. The brief description of the dataset/model set in CRK, EM, and TD in ECUME are given below.

2.3.1. Dataset for chemical reaction kinetics (CRK)

CRK mainly targets the gas phase reaction modes of Cs-I-B-Mo-O-H and Ru-N-O-H systems. CRK for the gas phase reaction consists of main elemental chemical reactions and their chemical reaction rate constants. Considering the bimolecular chemical reaction in the gas phase, A(g) + B(g) ↔ C(g) + D(g), the molar concentration of product species C(g) is expressed as:

$$\frac{\mathrm{d[C]}}{\mathrm{d}t} = k_\mathrm{f}[\mathrm{A}][\mathrm{B}] - k_\mathrm{r}[\mathrm{C}][\mathrm{D}] \tag{1}$$

where k_f and k_r are the forward and reverse chemical reaction rate constants, respectively; the elements in parentheses are their molar concentrations. The chemical reaction rate constant k_f is generally assumed to have the following Arrhenius-type temperature dependence:

$$k_\mathrm{f} = A(T)\exp\left(-\frac{E}{\mathrm{R}T}\right) = AT^n\exp\left(-\frac{E}{\mathrm{R}T}\right) \tag{2}$$

where R, T, and E are the gas constant, absolute temperature, and activation energy, respectively. Pre-exponential factor $A(T)$ is generally expressed as $A \times T^n$ in the right side of Equation (2), where n is the real number. The coefficients of these A, n, and E in chemical reaction rate constants are integrated as CRK for the gas phase reaction. The reverse chemical reaction rate constant is calculated using the equilibrium constant K_eq that can be expressed by enthalpy ΔH and entropy ΔS through the Gibbs free energy:

$$k_\mathrm{r} = \frac{k_\mathrm{f}}{K_\mathrm{eq}} = \frac{AT^n\exp\left(-E/\mathrm{R}T\right)}{\exp\left(-[\Delta H - T\Delta S]/\mathrm{R}T\right)} \tag{3}$$

CRK also targets the gas-solid phase reaction mode of Cs chemisorption onto SS and B-driven Cs and I re-vaporization. Although the gas-solid phase reaction is expressed as a complex reaction, the equation of chemical reaction rate constants k in the gas-solid phase reaction mode are basically the same as those in the gas phase reaction mode, as shown in Equation (2).

2.3.2. Elemental model set (EM)

EM targets the models of the Cs chemisorption onto SS and re-vaporization from chemisorbed compounds, B-driven Cs and I re-vaporization, and aerosol behavior and solubility of FP compounds. These models will be continuously improved and verified based on the latest fundamental experiments.

i) Chemical reactions

For the Cs chemisorption onto SS, the model proposed by Bowsher et al. (hereafter, Bowsher's model[28]) has been generally used in current SA analysis codes. In Bowsher's model, the first-order surface reaction rate constant, v_d, was used for each water-soluble and water-insoluble Cs deposits by accounting for the influence of temperature and atmospheric environments. In this model, the chemisorption amount per unit time unit area N is expressed as:

$$N = v_d C_g \tag{4}$$

where v_d is the surface reaction rate constant, and C_g is the concentration of species in the gas phase. v_d was expressed as an Arrhenius-type temperature dependence as:

$$v_d = A\exp\left(-\frac{E}{RT}\right) \tag{5}$$

where A is the pre-exponential factor, and E is the activation energy. The coefficients in Equation (5) were improved for CsOH chemisorption onto SS in ECUME based on the experiments that reproduced the Cs chemisorption onto SS under various chemical conditions.

However, in major SA analysis codes, the re-vaporization behavior can be modeled only for the deposit derived from condensation onto a wall[29], i.e., no models for the re-vaporization from the chemisorbed Cs. Therefore, the new re-vaporization model should be implemented in the SA analysis codes to reproduce re-vaporization with a chemical reaction such as B-driven Cs and I re-vaporization and the re-vaporization from Cs chemisorbed materials. In ECUME, considering its implementation in the current SA analysis codes, the model for the mass transfer with a chemical reaction will be implemented. The transported gas amount from the gas phase to the surface of solid per unit time unit area N is expressed using the mass transfer coefficient as:

$$N_w = k_g(C_\infty - C_w) \tag{6}$$

where C_w and C_∞ are the concentration of gas at the surface of a solid and the concentration of a gas bulk. Considering the bimolecular chemical reaction, A(g) + B(s) → C(g) + D(s), the reaction occurs only on the deposit surface. Thus, the gas amount of product species d[C]/dt is expressed using the fraction of reaction site on the deposit surface θ:

$$\frac{\mathrm{d[C]}}{\mathrm{d}t} = k_{\mathrm{f}} C_{\mathrm{w}} \theta \tag{7}$$

where k_{f} is the forward chemical reaction rate constant that will be integrated to determine the CRK of the gas-solid phase reaction mode. If the reaction proceeds in a steady state, N in Equation (6) corresponds to d[C]/dt in Equation (7). Therefore, the gas amount of product species d[C]/dt can be expressed using Equations (6) and (7) as:

$$\frac{\mathrm{d[C]}}{\mathrm{d}t} = \frac{C_{\infty}}{\left({}^{1}/_{k_{\mathrm{f}}\theta}\right)+\left({}^{1}/_{k_{\mathrm{g}}}\right)} \tag{8}$$

On the other hand, if the reaction can be assumed to be completed immediately, then C_{w} can be calculated using the equilibrium vapor pressure of C(g) shown in Equation (9). Thus, the gas amount of product species d[C]/dt can be expressed as Equation (10).

$$C_{\mathrm{w}} = \frac{p_{\mathrm{C(g)}}}{\mathrm{R}T} \tag{9}$$

$$\frac{\mathrm{d[C]}}{\mathrm{d}t} = k_{\mathrm{g}} \left(C_{\infty} - \frac{p_{\mathrm{C(g)}}}{\mathrm{R}T} \right) \tag{10}$$

The k_{f} and θ coefficients will be improved in ECUME based on experiments reproducing the re-vaporization under various chemical conditions. The equilibrium vapor pressure p in Equation (10) will be calculated using the thermodynamic dataset implemented in ECUME TD.

ii) Aerosol behavior

For the aerosol behavior, EM first targets the aerosol removal model by water droplet proposed by M. Ali et al.[30]. The removal efficiency of a single droplet η is calculated from inertial impaction mechanism, which is the function of the Stokes number. This phenomenon is more dominant for the particle size of 1 μm[31]. The impaction of single droplet efficiency[32] is defined as,

$$\eta = \left(\frac{\psi}{\psi+0.7} \right)^2 \tag{11}$$

where ψ[33] is expressed as

$$\psi = \frac{\rho_{\mathrm{p}} d_{\mathrm{p}}^2 \left(v_{\mathrm{p}} - v_{\mathrm{dr_i}} \right)}{9 \mu_{\mathrm{g}} d_{\mathrm{d}}} \tag{12}$$

where ρ_{p} is the particle density, d_{p}, and d_{dr} are the diameters of the particle and droplet, respectively, v_{p} and v_{dri} are the velocities of the particle and initial droplet, respectively, and μ_{g} is the viscosity of gas. Although most Cs and I compounds are soluble, this chemical property was not considered in this model. Therefore, the model shown in Equations (11) and (12) will be improved in ECUME by adding the coefficients related to the solubility of Cs and I compounds based on the experiments reproducing the interaction of CsI aerosol

with water droplets.

In addition, EM for aerosol behavior will target the models for deposition and resuspension, which are implemented to present the SA analysis codes.

iii) Aqueous phase behavior

For the evaluation of the FPs migration from fuel debris or deposit compounds through the aqueous phase, the dissolution rate of FPs into water is one of the essential parameters. The dissolution rate can be expressed via the Noyes-Whitney equation[34,35], as follow. This equation will be first applied for the Cs dissolution model from chemisorbed compounds in ECUME.

$$\frac{\mathrm{d}C_\mathrm{l}}{\mathrm{d}t} = S_\mathrm{p} k_\mathrm{a} (C_\mathrm{S} - C_\mathrm{l}) \tag{13}$$

where C_l is the concentration of the dissolved Cs at a given time t, S_p is the surface area of the solute particle, k_a is the dissolution rate constant, and C_S is the Cs concentration of the saturated solution. As a first step, $\mathrm{d}C_\mathrm{l}/\mathrm{d}t$ in the case of chemisorbed Cs deposit on the SS specimen will be evaluated by a long-term water elution test. The solubility concentration of Cs chemisorbed species will be also measured to calculate C_S in Equation (13).

2.3.3. Thermodynamic dataset (TD)

TD consists of heat capacity, $C_\mathrm{p}°$, entropy, $S°$, Gibbs energy function, $-(G° - H_{298}°) / T$, enthalpy increment, $H° - H_{298}°$, enthalpy of formation, $\Delta_\mathrm{f}H°$, and Gibbs energy of formation, $\Delta_\mathrm{f}G°$, for the elements and compounds associated with nuclear materials. The superscript "°" means the standard state pressure of 1 bar (0.1 MPa). The subscript "$_\mathrm{f}$" means the formation quantities of compounds. TD will be utilized not only to improve CRK and EM but also for the thermodynamic assessment of the reactor under an SA. The thermodynamic data of new compounds observed in the experiments will be derived from the experiments, such as high temperature Knudsen Effusion Mass-Spectrometry, and will be estimated by an empirical method or an *ab-initio* calculation if the experimental data are not available.

For example, if CsI and its constituent elements Cs and I are in their standard state or at 1 bar are solid, liquid, and gaseous phases, respectively, the formation reaction of CsI is expressed by the following equation:

$$\mathrm{Cs(l)} + 0.5\ \mathrm{I_2(g)} = \mathrm{CsI(s)} \tag{14}$$

the corresponding value for the standard enthalpy of formation, denoted by $\Delta_\mathrm{f}H°$(CsI,s), may be obtained by:

$$\Delta_\mathrm{f}H°(\mathrm{CsI,s}) = H°(\mathrm{CsI,s}) - H°(\mathrm{Cs,l}) - 0.5\ H°(\mathrm{I_2,g}). \tag{15}$$

To calculate these thermodynamic data at any desired temperature, it is essential to know the enthalpy

of formation and standard entropy at 298.15 K, $\Delta_f H_{298}°$, $S_{298}°$, and the variation of heat capacity with temperature of all phases of interest, $C_p°$. Thus, $\Delta_f H°$ and $\Delta_f G°$ may be calculated using the values of $\Delta_f H_{298}°$, $S_{298}°$, and $C_p°$, as follows:

$$\Delta_f H°(\text{formed compound}) = \Delta_f H_{298}°(\text{formed compound}) + H° - H_{298}°(\text{formed compound}) - \sum\{H° - H_{298}°(\text{constituent element})\}, \quad (16)$$

$$\Delta_f G°(\text{formed compound}) = \Delta_f H_{298}°(\text{formed compound}) - T\,[-(G° - H_{298}°)/T\ (\text{formed compound}) - \sum\{-(G° - H_{298}°)/T\ (\text{constituent element})\}], \quad (17)$$

where, for example, if two phase transitions of α → β and β → γ exist and the temperature is higher than the transition temperature of β→γ,

$$H° - H_{298}° = \int_{298.15}^{T(\alpha\to\beta)} C_p°(\alpha)\mathrm{d}T + \Delta_{tr}H°(\alpha\to\beta) + \int_{298.15}^{T(\beta\to\gamma)} C_p°(\beta)\,\mathrm{d}T + \Delta_{tr}H°(\beta\to\gamma) + \int_{T(\beta\to\gamma)}^{T} C_p°(\gamma)\,\mathrm{d}T, \quad (18)$$

$$S° = S_{298}° + \int_{298.15}^{T(\alpha\to\beta)} \frac{C_p°(\alpha)}{T}\mathrm{d}T + \Delta_{tr}S°(\alpha\to\beta) + \int_{T(\alpha\to\beta)}^{T(\beta\to\gamma)} \frac{C_p°(\beta)}{T}\mathrm{d}T + \Delta_{tr}S°(\beta\to\gamma) + \int_{T(\beta\to\gamma)}^{T} \frac{C_p°(\gamma)}{T}\mathrm{d}T, \quad (19)$$

$$-(G° - H_{298}°)/T = S° - (H° - H_{298}°)/T, \quad (20)$$

where $\Delta_{tr}H°$ and $\Delta_{tr}S°$ are the phase transition enthalpy and entropy, respectively.

In general, for condensed phases, the experimental values of $\Delta_f H_{298}°$, $S_{298}°$, and $C_p°$ can be obtained from calorimetric, electromotive force, and vapor pressure measurements, respectively. For gases, $\Delta_f H_{298}°$ and the thermodynamic functions, such as $C_p°$ and $S°$, are normally obtained from vapor pressure measurements and molecular parameters by statistical mechanical calculations using the following relationships:

$$C_p° = \mathrm{R}\frac{\mathrm{d}}{\mathrm{d}T}\left(T^2\frac{\mathrm{d}Q/\mathrm{d}T}{Q}\right) \quad (21)$$

$$S° = \mathrm{R}\left(T\frac{\mathrm{d}Q/\mathrm{d}T}{Q} + \ln Q\right) \quad (22)$$

$$-(G° - H_0°)/T = \mathrm{R}\ln Q \quad (23)$$

$$H° - H_0° = \mathrm{R}T^2\frac{\mathrm{d}Q/\mathrm{d}T}{Q} \quad (24)$$

where Q is the partition function:

$$Q = Q_{\mathrm{t}} \sum_i \; Q_{\mathrm{e}}^i Q_{\mathrm{v}}^i Q_{\mathrm{r}}^i \tag{25}$$

Q_{t} is the translational partition function, and Q_{e}^i, Q_{v}^i, and Q_{r}^i are the electronic, vibrational, and rotational partision function of the i-th state. If only the ground state is considered, the abovementioned equation can be written as:

$$Q = Q_{\mathrm{t}} Q_{\mathrm{e}} Q_{\mathrm{v}} Q_{\mathrm{r}}. \tag{26}$$

The following equations for the individual partition functions are used:

$$Q_{\mathrm{t}} = \frac{\sqrt[3]{2\pi m \mathrm{k_B} T}}{\mathrm{h}^3} V \tag{27}$$

where m is the molecular mass, $\mathrm{k_B}$ is the Boltzmann constant, h is the Planck constant, and V is the molar gas volume,

$$Q_{\mathrm{e}} \; = \sum_i \; g_i \mathrm{e}^{\frac{\varepsilon_i}{\mathrm{k_B} T}} \tag{28}$$

where g_i is the quantum (or statistical) weight of the i-th electronic state; the quantity is the product of the spin multiplicity and state degeneracy of the electronic level under consideration, and ε_i is i-th electron energy level,

$$Q_{\mathrm{v}} = \frac{1}{1-\mathrm{e}^{-\mathrm{u}}} \tag{29}$$

where $u = c_2(\omega_{\mathrm{e}} - 2\omega_{\mathrm{e}}\chi_{\mathrm{e}}) / T$ for the anharmonic oscillation model, $u = c_2\omega / T$ for the harmonic oscillator, c_2 is the second radiation constant, ω_{e} is the vibrational fundamental for an infinitesimal amplitude, $\omega_{\mathrm{e}}\chi_{\mathrm{e}}$ is vibrational anharmonicity constant, and ω is the fundamental vibrational frequency of a harmonic oscillator.

$$\text{Rotation for diatomic molecules: } \; Q_{\mathrm{r}} = \beta^{-1}\left(1 - \frac{\beta}{3} - \frac{\beta^2}{15} + \frac{4\beta^3}{315}\right) \tag{30}$$

where $\beta = 8\pi^2 I \mathrm{k_B} T / \sigma \mathrm{h}$ for the rigid rotor model, $\beta = T / (\mathrm{B_e} - \alpha_{\mathrm{e}} / 2)$ for the non-rigid rotor model, σ is the symmetry number of molecules, I is the moment of inertia, $\mathrm{B_e}$ is the rotational constant, and α_{e} is the first-order rotation-vibration interaction constant.

$$\text{Rotation for polyatomic molecules (rigid rotor model only): } \; Q_{\mathrm{r}} = \frac{8\pi^2 \sqrt[3]{8\pi^3 I_{\mathrm{A}} I_{\mathrm{B}} I_{\mathrm{C}}}}{\sigma \mathrm{h}^3} \sqrt[3]{\mathrm{k_B} T} \tag{31}$$

where I_{A}, I_{B}, and I_{C} are the principal moments of inertia of a polyatomic molecule.

2.4. Schedule

Figure 2 shows the schedule for the construction of ECUME. ECUME will be continuously improved, and ECUME for the SA of LWR will be created by 2021. The outcome based on ECUME will be timely reflected in both the 1F decommissioning work through the improvement of source term and the enhancement of LWR safety after the 1F SA.

Table 1 Contents of the final version of the FP chemistry database ECUME

Phenomenon / behavior Chemical system		CRK Chemical reaction rate constant	EM Element model	TD Thermodynamic data
Chemical reaction in gas phase	**Changes in speciation (Cs-I-Mo-B-O-H system)**	**More than 200 elementary reactions**	—	**$CsBO_2$(g)**, $Cs_2B_4O_7$(s), and CsB_3O_5(s)
	Changes in speciation (Ru-N-O-H system)	**More than 100 elementary reactions**		RuO(g), RuO_2(g), RuO_3(g), and RuO_4(g)
	Changes in speciation (TBD: Sr, Ba-containing system)			—
Chemical reaction for solid–gas phase	Cs and I re-vaporization by B (and Mo) vapor species (Cs-I-B-Mo-O-H system)	Complex reaction of CsI(s) + HBO_2(g,s) → $CsBO_2$(s) + HI(g)	**n^{th} order reaction model with reaction kinetics constant composed of Arrhenius equation,** or Mass transfer model with partial pressure of gas species	HBO_2(g)
	Cs chemisorption onto SS and re-vaporization (Cs-Fe-Si-O-H system)	Complex reaction of CsOH(g) + (Fe, Si) → Cs-Si-Fe-O compound → Cs compd.(g)		$Cs_2Si_2O_5$(s,l), **$Cs_2Si_4O_9$(s,l)**, **$CsFeSiO_4$(s)**, and $CsFeSi_2O_6$(s)
	Sr (and Ba) chemisorption (Sr-Cl-O system)	—	TBD (same as Cs chemisorption)	—
	Ru reaction with a wall	TBD	TBD	TBD
Aerosol behavior	Detailed Aerosol deposition behavior (Cs-I-O-H system)	—	TBD (model of aerosol deposition on the crack)	—
	Aerosol removal by droplets (filtered vent system) (Cs-I-O-H system)		Model of aerosol removal by droplets	
	Resuspension of aerosol (Cs-I-O-H system)		TBD (model using critical friction velocity)	
Aqueous phase behavior	Leaching of Cs compounds (Cs-I-Mo-B-Fe-Si-O system)	Cs compd. (s) → Cs or Cs complex ions	Noyes-Whitney model	CsI(s), Cs_2MoO_4(s), Cs-B-O compd., Cs-Fe-Si-O compd

Underline; Included in this version of ECUME, TBD: to be determined

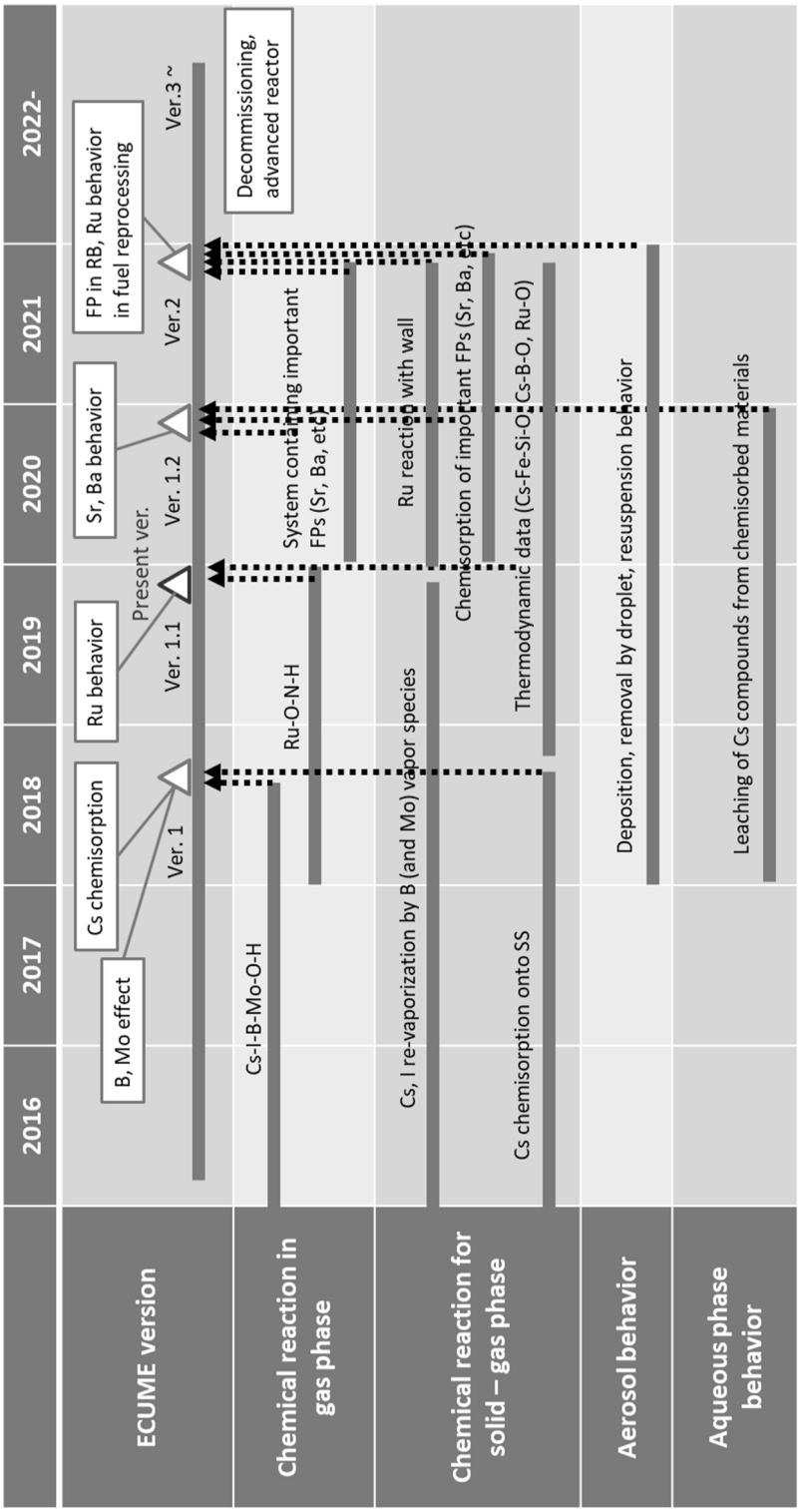

Figure 2 Schedule for the creation of ECUME

3. Dataset for chemical reaction kinetics (CRK)

3.1. Overview

CRK is a dataset of chemical reaction kinetic constants for possible chemical reactions in LWR SA. CRK for the gas phase reaction is based on either the literature data or, if the literature data are not available, on calculation results using a combinational method of *ab-initio* calculation with statistical physics[18]. By comparing the species calculated using CRK for a period of time that is sufficiently long to regard it as the chemical equilibrium condition to those by chemical equilibrium calculations, it was confirmed that major reaction pathways were not excluded from the dataset[18]. This version of ECUME is equipped with CRK for the gas phase reactions of Cs-I-B-Mo-O-H and Ru-N-O-H systems.

CRK in the gas-solid phase will be included in the future version of ECUME. CRK in the gas-solid phase can be obtained based on the separate-effect experiments that reproduce the FP behavior with various chemical conditions because it is difficult to obtain the chemical reaction kinetic constants in the same way as those in the gas phase.

CRK can be directly applied to the mechanistic codes such as the SOPHAEROS module in the ASTEC code[36], which can evaluate the FP chemistry with the reaction kinetics.

3.2. Modeling method

The dataset of coefficients of A, n, and E in chemical reaction rate constants in Equation (2) was prepared either by referring to the literature or, if the literature data were not available, by calculation results using a combinational method of *ab-initio* calculation with statistical physics [18]. If more than two data sets were available for one chemical reaction, one data set was selected using the following criteria:

- Year of publication:
  Latest data were adopted. However, if they were clearly inappropriate (including misprints), other data were adopted.
- Estimation method:
  There are two types of estimation methods for the chemical reaction rate constants. One type is the direct estimation of the chemical reaction, and the other type is indirect estimation by the analogies from other similar reactions. The data estimated by the former direct method was adopted if there are two types of estimation methods.
- Temperature range:
  The data that correspond to or are near the temperature range in this study, 400–2500 K, were adopted.
- Third body chemical species:
  The term “third body” refers to gas species in the atmosphere that do not participate in chemical reactions. Third body is usually represented by the symbol “M” in the chemical reaction formula. It can add energy to or remove energy from the reactants. In case that there were several literature data given for different third body gas species, the priority was given to the data for Ar, followed by H_2O,

then N_2, considering the atmospheric conditions of future experiments for the FP release and transport[17,37].

If no literature data were available for the dataset, the data were estimated by theoretical calculations. The calculations were made by a combinational method of *ab-initio* calculation using the NWChem software[38], for example, with statistical physics. Calculation conditions of the *ab-initio* calculation are summarized in Table 2. The path of each chemical reaction was determined by Nudged Elastic Band method which is known to be effective for finding a minimum energy path of a gas phase reaction[39]. If a transition state lies on a chemical reaction process, transition state theory (TST) was adopted. Given a bimolecular chemical reaction A(g) + B(g) ↔ C(g) + D(g), the reaction rate constant can be calculated by the TST as:

$$k_{\mathrm{f}} = \left(\frac{\mathrm{R}T}{\mathrm{h}}\right)\frac{Q_{\mathrm{TS}}(T)}{Q_{\mathrm{A}}(T)Q_{\mathrm{B}}(T)}\exp\left(-\frac{E}{\mathrm{R}T}\right) \tag{32}$$

where h is Planck's constant, $Q_{\mathrm{A}}(T)$, $Q_{\mathrm{B}}(T)$, and $Q_{\mathrm{TS}}(T)$ are the total partition functions for chemical species of A(g), B(g), and the transition state, respectively. The total partition function $Q(T)$ can be written in terms of the translational ($Q_{\mathrm{t}}(T)$), rotational ($Q_{\mathrm{r}}(T)$), and vibrational ($Q_{\mathrm{v}}(T)$) partition functions as follows:

$$Q(T) = Q_{\mathrm{t}}(T)Q_{\mathrm{r}}(T)Q_{\mathrm{v}}(T). \tag{33}$$

The activation energy E can be calculated as the energy difference between the transition and initial states.

For example, for reactions that involve monotonic energy change without transition states, which typically occur for the dissociation of a diatomic molecule such as AB(g) + M ↔ A(g) + B(g) + M, the Rice–Ramsperger–Kassel (RRK) theory[40,41] was adopted. By assuming that the total pressure is much higher than the partial pressure of reactants, the reaction rate constant can be calculated based on the RRK theory as:

$$k_{\mathrm{f}} = \upsilon \exp\left(-\frac{E}{\mathrm{R}T}\right) \tag{34}$$

where υ is the vibrational frequency of the reactants.

$Q_{\mathrm{A}}(T)$, $Q_{\mathrm{B}}(T)$, $Q_{\mathrm{TS}}(T)$, υ, and E in Equations (32) and (34) were calculated by NWChem at 298 K and at each 20 K from 300 K to 4000 K according to the abovementioned chemical reaction types. Using these calculated parameters, the reaction rate constants k can be obtained using either Equation (32) or (34) at each temperature. The fitting of the calculated k by Equation (2) finally gave the coefficients of A and n. Additional details can be found in ref. [18]. The thermodynamic data for calculating the reverse chemical reaction rate constants was prepared based on the SGTE substances database [42]. The dataset of CRK and thermodynamic data is shown in appendix A.

3.3. Verification

The species calculated using CRK for a time period that is sufficiently long to regard it as the chemical equilibrium condition were compared to those by chemical equilibrium calculations to make sure that major reaction pathways were not missing in the dataset. Table 3 lists the conditions for the chemical reaction calculations. The calculations were carried out by assuming that spatially homogeneous chemical reactions occur in a closed system at several representative temperatures from 1000 K to 2500 K. The comparison of Cs-I-B-O-H, Cs-I-B-Mo-O-H, and Ru-N-O-H systems is shown in Figure 3, Figure 4**,** and Figure 5, respectively. The agreements are good for these systems including $CsBO_2$ and Cs_2MoO_4, which are important chemical species from the viewpoint of the Cs chemistry[43,44,45]. Although the reliability of CRK should be evaluated and improved using experimental results, these results show that, at least, CRK is useful for evaluating the FP chemistry considering the kinetic limitation effect.

Table 2 *Ab-initio* calculation conditions for the chemical reaction rate constants

	Conditions	Ref.
Basis function	(Mo-containing species)	
	def2-SVP	[46]
	for structural optimization	
	& Nudged Elastic Band method	
	def2-TZVPD	[47]
	for vibration analysis	
	(Others)	
	def2-SVP	[46]
	for structural optimization	
	& Nudged Elastic Band method	
	& vibration analysis	
Core electron	def2-ECP (for Cs, I, Mo)	[48,49,50]
Calculation method	Hybrid-DFT method (M06-2X)	[51]

Table 3 Conditions for the chemical reaction calculations

	Conditions
Spatial condition	Closed and homogeneous
Pressure (MPa)	0.1
Temperature (K)	1000 - 2500
Initial amounts (mol)	
Cs-I-B-Mo-O-H system	
Ar	0.045
H_2O	0.045
CsI	1.0×10^{-8}
H_3BO_3	1.0×10^{-8}
MoO_3	1.0×10^{-8}
Ru-N-O-H system	
N_2	0.4
H_2O	0.5
O_2	0.1
RuO_2	1.0×10^{-8}

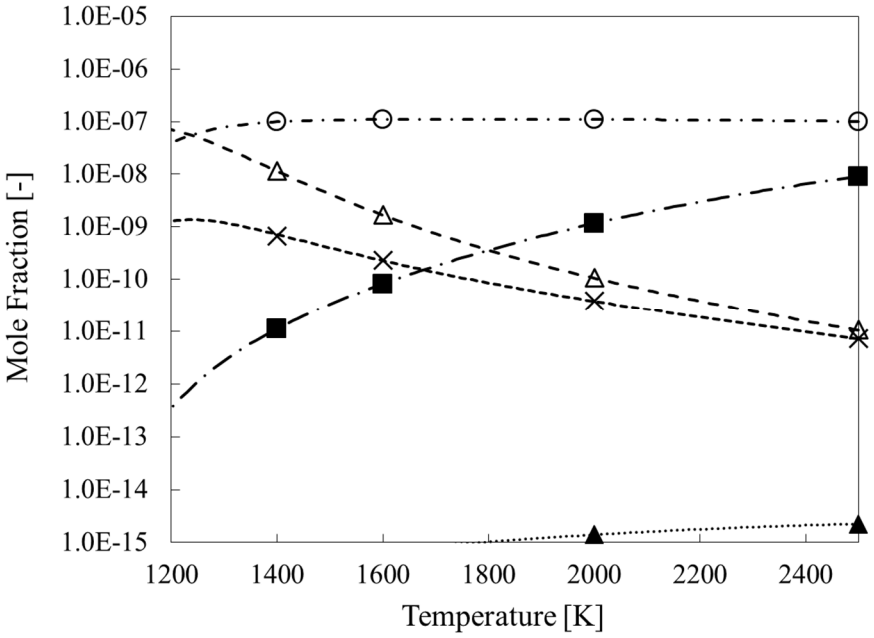

Figure 3 Comparison of the chemical equilibrium composition of representative Cs-I-B-O-H species (symbols: results of the chemical reaction calculation, lines: results of the chemical equilibrium calculation)[18)]

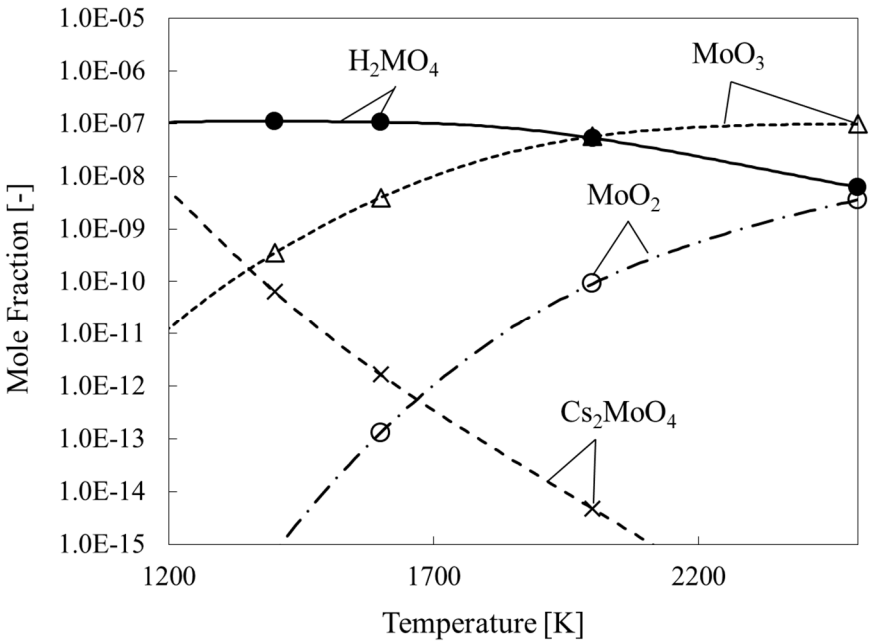

Figure 4 Comparison of the chemical equilibrium composition of representative Cs-I-B-Mo-O-H species (symbols: results of the chemical reaction calculation, lines: results of the chemical equilibrium calculation)[18)]

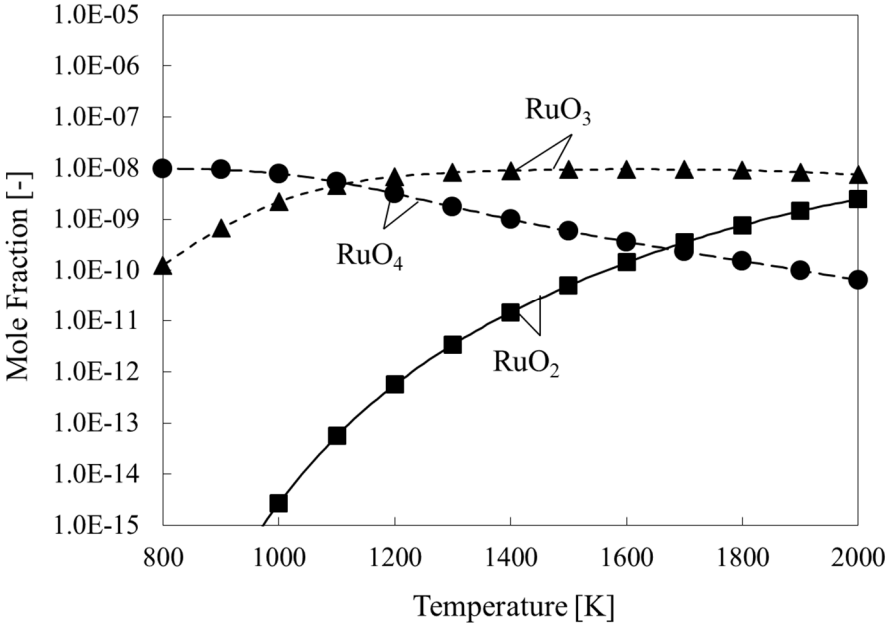

Figure 5 Comparison of the chemical equilibrium composition of representative Ru-N-O-H species (symbols: results of the chemical reaction calculation, lines: results of the chemical equilibrium calculation)

4. Elemental model set (EM)

4.1. Overview

EM is established based on the separate-effect experiments that reproduce FP behaviors with various chemical and thermo-hydraulic conditions as parameters. The model coefficients are determined by fitting the experimental results to the model equations that are newly determined by considering major factors for the FP behaviors.

EM is an elemental model set for the FP chemical/physical behaviors in the SA of LWR. The future version of EM will include the models for aerosol and aqueous phase behavior of dissolved Cs compounds.

This version of ECUME included EM for the CsOH chemisorption onto SS. Currently, Bowsher's model for CsOH chemisorption onto SS is incorporated into the SA analysis code[28]. However, Bowsher's model has a large uncertainty primarily because of the simple treatment of chemical factors; thus, it is insufficient for considering various chemical conditions along with the SA progression at 1F SA. Therefore, the CsOH chemisorption model in ECUME was improved to treat the various influencing chemical factors. The improved chemisorption model provides a more accurate estimation of a possible localization of water-insoluble and stable Cs deposits at the upper part of RPV[28,52,53] at 1F.

4.2. Modeling method

4.2.1. Experimental investigation of influencing chemical factors

The influencing chemical factors on the CsOH chemisorption behavior were investigated by a series of CsOH chemisorption tests in which the SS type-304 (SS304) specimens were reacted with the CsOH vapor using the conditions and parameters shown in Table 4[54]. The test results were evaluated using the surface reaction rate constant, v_d, which is shown in Equation (4)[28]. v_d can be calculated by experimental results of the CsOH chemisorption amount per unit time unit area N [μg Cs/cm^2/s] and the concentration of CsOH in the gas phase C_g [μg/cm^3] using Equation (4). Of note, v_d for the water-insoluble Cs deposit depended not only on the temperature, as already known[53,28], but also on the Si content in SS304, as shown in Figure 6, and on CsOH concentration in the gaseous phase as shown in Figure 7. Furthermore, it was determined that v_d had the $y = \mathrm{b}x^{-\mathrm{a}}$ type of dependence on C_g.

4.2.2. Establishment of an improved CsOH chemisorption model

To consider the influence of the Si content in SS304 and CsOH concentration in the gaseous phase, a theory of mass transfer with a chemical reaction was used to improve Bowsher's model[55]. Considering the mass transfer at the gas-solid interface, the surface reaction rate constant, v_d, can be described using the following equation:

$$v_{\mathrm{d}} \cong H_{\mathrm{S}}\sqrt{k"D_{\mathrm{S}}C_{\mathrm{B}}} \tag{35}$$

where H_S is the solubility coefficient, k'' is the second-order reaction rate constant [1/s/wt.%], D_S is the diffusion coefficient of Cs reactant species in the solid phase [cm^2/s], and C_B is the concentration of reactant species of solute B in the solid phase, which is the Si content in SS304 in this study [wt.% Si]. Normally, H_S, k'', and D_S can be assumed to have an Arrhenius-type temperature dependence. In this study, it was also assumed that H_S had the $y = bx^{-a}$ type dependence on C_g. Consequently, Equation (36) was considered as the modified CsOH chemisorption model that considers the influence of the Si content in SS304, C_B, and CsOH concentration in the gaseous phase, C_g:

$$v_d = \frac{A(k''D_SH_S)}{C_g{}^{x(H_S)}}\sqrt{C_B}\exp\left(-\frac{B(k''D_SH_S)}{T}\right) \quad (36)$$

where $A(k''D_SH_S)$, $B(k''D_SH_S)$, and $x(H_S)$ are the fitting parameters. The fitting parameters of Equation (36) were determined from the experimental v_d. Thus, Equation (37) was obtained as the modified CsOH chemisorption model:

$$v_d = \frac{7.027\pm2.794}{C_g^{0.5225\pm0.0597}}\sqrt{C_B}\exp\left(-\frac{6552\pm1197}{T}\right). \quad (37)$$

The ranges in application of this model are from 1073 K to 1273 K, 0.2 μg to 20 μg of CsOH /cm^3, in the H_2O-containing atmosphere, and 0.1 wt.% to 4.9 wt.% of Si content.

4.3. Verification

Figure 8 shows the comparison results of the consistency of calculated v_d with experimental v_d between the improved model and Bowsher's model. The calculated v_d from the improved model agreed with the experimental v_d better than those from Bowsher's model. Twofold standard deviations of logarithm of v_d, 2σ, for our improved model and for Bowsher's model were 0.513 and 1.43, respectively. Therefore, it was determined that the uncertainty of the improved model was nearly one order of magnitude smaller than that of Bowsher's model because our improved model considered the effects not only on temperature but also on the CsOH concentration in the gaseous phase and Si content in SS304.

Table 4 Parameters for the CsOH chemisorption test

Parameters	Conditions
Temperature [K]	873-1273
Atmosphere	Ar-5%H_2
	Ar-5%H_2-5%H_2O
	Ar-4%H_2-20%H_2O
CsOH concentration in gas phase [μg/cm^3]	0.2-20
Deposition time [min]	180-360
Si content in SS304 specimen [wt.%]	0.1 - 4.9

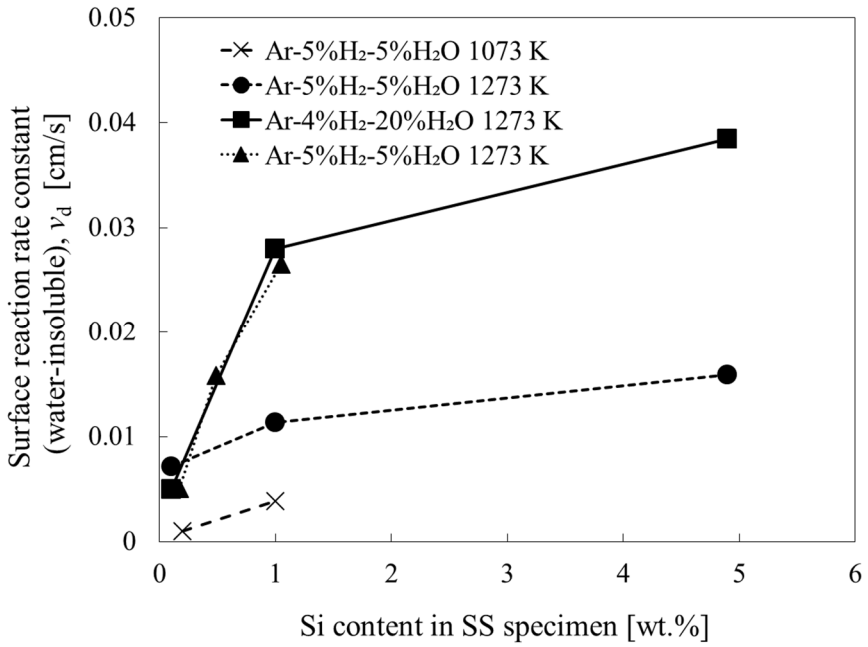

Figure 6 Dependence of the surface reaction rate constant v_d for water-insoluble Cs deposit on the Si content in the SS304 specimen[54)]

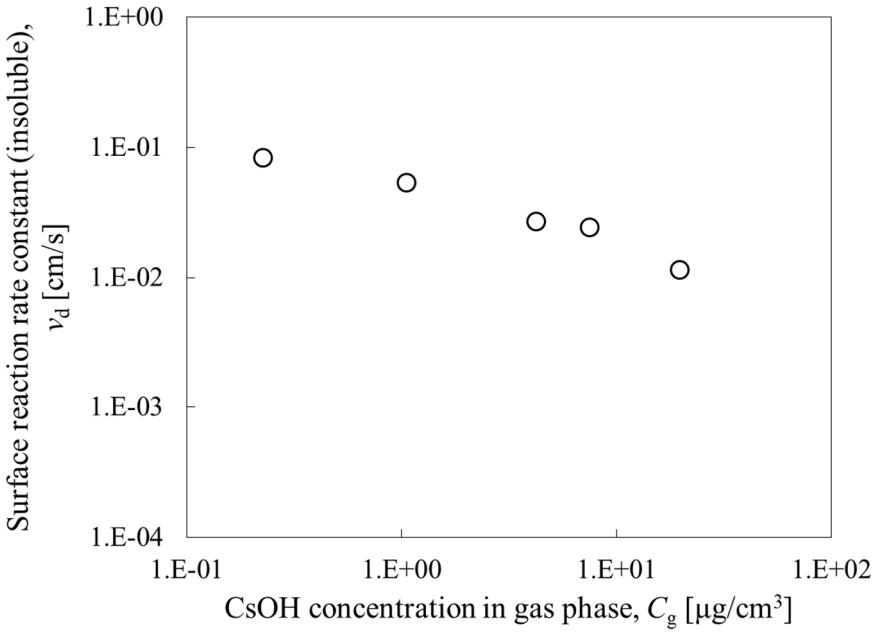

Figure 7 Dependence of the surface reaction rate constant v_d for the water-insoluble Cs deposit on the CsOH concentration in the gas phase C_g[54)]

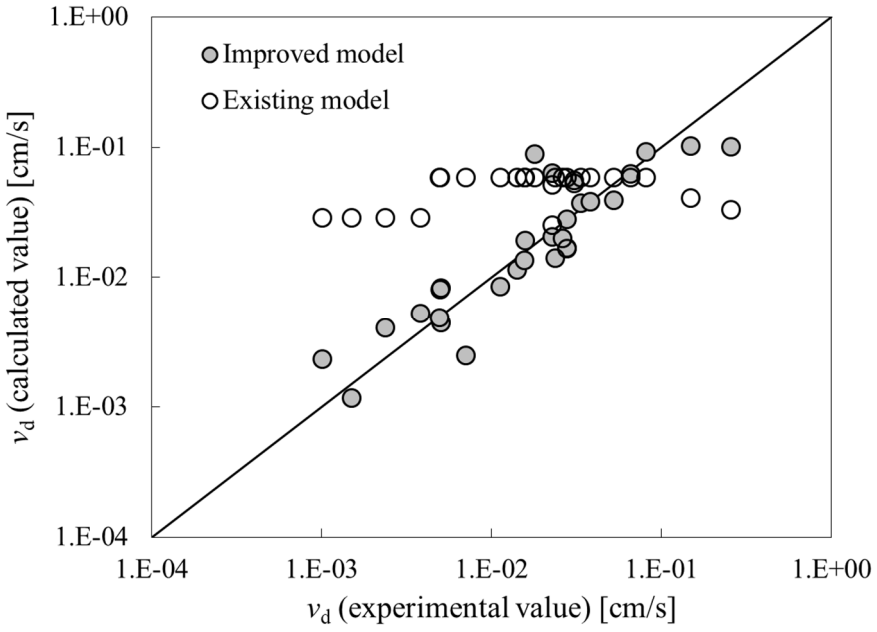

Figure 8 Comparison of the consistency of calculated v_d with the experimental v_d between the improved and Bowsher's models[55)]

5. Thermodynamic dataset (TD)

5.1. Overview

Currently, $CsBO_2$ vapor species and solids, $Cs_2Si_4O_9$ and $CsFeSiO_4$, are the target compounds for the first version of TD because thermodynamic properties of these compounds are not well-known but essential to understand the Cs release and transport behaviors, including the Cs chemisorption behaviors onto SS.

5.2. Modeling method

No available values on thermal properties of $CsFeSiO_4$ are provided in the literature. In this study, we proposed a first estimation of the thermal properties of this substance by computational chemistry through density-functional theory (DFT) calculations for the structural and energetic properties coupled with statistical physics to derive the thermodynamic functions. To establish the computational methodology, the structural, and thermal properties of $Cs_2Si_4O_9$ were calculated and compared with the available thermodynamic data.

DFT calculations were carried out with the Vienna *Ab-initio* Simulation Package (VASP)[56,57,58,59]. The wave function is expanded in a plane wave basis set, and the electron-ion interactions are described using the projector augmented plane wave potentials [60, 61]. The calculations were performed with the gradient-corrected exchange correlation functional of Perdew, Burke, and Ernzerhof (PBE)[62], with a smearing of 0.2 eV, with its relative pseudopotentials. The solution of the Kohn-Sham equations was improved self-consistently until a difference lower than 10^{-8} eV was obtained between successive iterations. To properly account for the localization of the Fe valence 3d electrons, we calculated iron-containing substances with Hubbard correction[63] using U = 3 eV and J = 0.0 eV to follow the recommendation using the fitted elemental-phase reference energy (F.E.R.E) methodology from Lany et al.[64]. Full structural optimizations were performed using a conjugate-gradient algorithm until the forces on atoms were lower than 0.001 eV/Å. The computational parameters of our target substances (i.e., k-mesh sampling and cutoff energy) are shown in Table 5 following previous investigations by Miradji et al.[65] and only differing for the energy cutoff to avoid the mathematical artifact in phonon calculations. The DFT calculations of $CsSiFeO_4$ prototypes were obtained in the antiferromagnetic (AFM) configuration; this latter magnetic state is the most stable, as has been reported in the previous study[65]. Visualizations of crystal structures and geometric parameters were obtained with the VESTA package[66].

In this study, vibrational properties and thermodynamic functions were calculated within the framework of the harmonic approximation. The difference between enthalpy and energy (pV) was neglected. This is a reasonable approximation for solids at atmospheric pressure and for temperatures considerably lower than 1000 K (order of magnitude of temperatures in our reproductive tests of Cs chemisorption). We calculated the phonon density of state ($g(\omega)$) within the small displacement methods using the VASP package[56,57,58,59] to calculate each displacement. The stabilities of the solid structures were confirmed by the absence of imaginary vibration modes in the phonon spectra. To calculate the thermodynamic properties, the following relationships were used:

$$E_{\mathrm{ZPE}} = \int_0^{\infty} \frac{1}{2} \mathrm{g}(\omega) \hbar\omega \mathrm{d}\omega \tag{38}$$

$$H_T - H_0 = \int_0^{\infty} \mathrm{g}(\omega) \hbar\omega \mathrm{n}(\omega) \mathrm{d}\omega \tag{39}$$

$$S_T = \mathrm{k_B} \int_0^{\infty} \mathrm{g}(\omega) \left(\frac{\hbar\omega}{\mathrm{k_B}T} \mathrm{n}(\omega) - \ln\left(1 - e^{\frac{\hbar\omega}{\mathrm{k_B}T}}\right) \right) \mathrm{d}\omega \tag{40}$$

$$\mathrm{n}(\omega) = \left(e^{\frac{\hbar\omega}{\mathrm{k_B}T}} - 1\right)^{-1} \tag{41}$$

where E_{ZPE} is the zero-point energy, $H_T - H_0$ is the enthalpy increment, and S_T is the vibrational entropy. The Phonopy software[67] was used to extrapolate the thermodynamic data from the calculation of force constants obtained for all displacements. To select the most stable prototype for Cs silicate substances, the standard enthalpy of formation of all candidates at 0 K was derived using the following equation:

$$\Delta_{\mathrm{f}} H_0\left(\mathrm{A}_x\mathrm{B}_y\right) = E\left(\mathrm{A}_x\mathrm{B}_y\right) - xE(\mathrm{A}) - yE(\mathrm{B}) \tag{42}$$

where $\mathrm{A}_x\mathrm{B}_y$ represents $CsFeSiO_4$ or $Cs_2Si_4O_9$, and A, B represent Cs, Fe, Si, and O_2 in their reference state. For Cs, Fe, and Si, the elements standard enthalpy in the solid phase was chosen, and O_2 dimer species in the gaseous phase was used. To reduce self-consistent error induced by DFT for semiconducting materials, the F.E.R.E corrections were applied to the derived heat of formation[64]. For the standard enthalpies at room temperature, the zero-point correction energy (ZPE) and enthalpy increment were added to Equation (42). The Gibbs free energy of formation was deduced from the standard enthalpy of formation, as expressed in the following equation:

$$\Delta_{\mathrm{f}} G_{298}\left(\mathrm{A}_x\mathrm{B}_y\right) = \Delta_{\mathrm{f}} H_{298}\left(\mathrm{A}_x\mathrm{B}_y\right) - T\Delta_{\mathrm{f}} S_{298}\left(\mathrm{A}_x\mathrm{B}_y\right). \tag{43}$$

For Cs, Fe, Si, and O_2, the thermal corrections above 298.15 K were obtained from the literature.

5.3. Verification

The recommended values and uncertainties of thermodynamic data in TD were determined from the second- and third-law analyses[68] if the Gibbs energy function, $-(G^\circ - H_{298}^\circ) / T$, for the reactants and products were available. More specifically, the uncertainty of thermodynamic data was evaluated from the difference between the second- and third-law values of the enthalpy in a reaction, and the recommended values were selected based on the thermodynamic dataset with the smallest difference between the second- and third-law values. The second- and third-law values of the reaction enthalpy can be calculated using the following equations, respectively:

$$\Delta_r H_{298}°(\mathrm{2nd}) = -\mathrm{R}\frac{\mathrm{d}(\ln K)}{\mathrm{d}\left(\frac{1}{T}\right)} - [\sum\{H° - H_{298}°(\mathrm{products})\} - \sum\{H° - H_{298}°(\mathrm{reactants})\}] \quad (44)$$

$$\Delta_r H_{298}°(\mathrm{3rd}) = -\mathrm{R}T \ln K - T\,[\sum\left\{\frac{-(G° - H_{298}°)}{T\ (\mathrm{products})}\right\} - \sum\{\frac{-(G° - H_{298}°)}{T\ (\mathrm{reactants})}\}] \quad (45)$$

where R is the gas constant, and K is the equilibrium constant for the reaction.

Regarding thermodynamic data, uncertainties of the thermodynamic data are marked as A, B, C, and D, where A represents good quality (generally better than 1%), B represents medium quality (1–5%), C represents poor quality (5–10%), and D is mainly based on estimates.

5.3.1. Gaseous cesium metaborate [$CsBO_2$(g)]

According to the compilation of thermodynamic data for reactor materials and compounds of FP elements[69], the thermodynamic data for $CsBO_2$(g) is determined to be of poor quality. However, regarding the Gibbs energy function for $CsBO_2$(g), there was only approximately a 0.1% difference between the values given by the compilation[69] and those derived from the latest experimental data on molecular constants of $CsBO_2$[70] despite the maximum difference of approximately 20% among all molecular constants[71]. Therefore, the Gibbs energy function of $CsBO_2$(g) can be regarded as a good quality. However, there were greater than 5% differences between the second- and third-law values of sublimation enthalpy of $CsBO_2$ at 298.15 K before our study. Thus, the equilibrium vapor pressure measurement of $CsBO_2$ was carried out using a Knudsen effusion mass spectrometer to obtain a reliable thermodynamic data of $CsBO_2$(g). Thus, the deference between the second- and third-law values of sublimation enthalpy of $CsBO_2$ was reduced up to 0.6%[72], and the thermodynamic data of $CsBO_2$(g) can be marked as “A”.

The recommended values of the thermodynamic data of $CsBO_2$(g) were calculated from the following molecular parameters:

bent molecule, r(Cs–O) = 0.269 nm, r(B–O) = 0.1298 nm, r(B=O) = 0.1219 nm, ∠(Cs–O–B) = 125°,
vibration frequencies: 1935, 1045, 632, 588, 233, 57 cm^{-1},
I_A, I_B, I_C = 1.69▪10^{-134} kg^3▪m^6, σ=1.
ground state, g_0 = 1

Figure 9 shows the equilibrium vapor pressures of $CsBO_2$ derived from the recommended thermodynamic data, together with the experimental data given by Nakajima et al. [72], Biswas and Mukerji[73], and Cordfunke et al.[74]. The data of TD for $CsBO_2$ is shown in Appendix B.

5.3.2. Solid cesium silicate [$Cs_2Si_4O_9$(s)]

The heat capacity above room temperature was obtained from enthalpy increment measurements using a drop calorimeter in the temperature range from 475 K to 825 K by Ball et al.[75]. These enthalpy increments were fitted by the equation:

$$\{H^\circ - H_{298}{}^\circ\}\mathrm{J/mol} = 367.1725(\mathrm{T/K}) + 0.505379\times10^{-3}(\mathrm{T/K})^2 + 114.205\times10^{5}(\mathrm{T/K})^{-1} - 147821.9 \quad (46)$$

The enthalpy of formation was determined by Cordfunke and Ouweltjes[76] using solution calorimetry. The enthalpy of formation was determined as:

$$\Delta_f H^\circ(298.15\ \mathrm{K}) = -(4297.6 \pm 5.4)\ \mathrm{kJ/mol} \quad (47)$$

The entropy was determined in our study. The heat capacity between 1.9 K and 302 K was determined using a thermal-relaxation calorimeter[77]. The entropy was derived from the following measurements:

$$S^\circ(298.15\ \mathrm{K}) = 322.1 \pm 1.3\ \mathrm{J/K/mol} \quad (48)$$

Thus, the recommended values of the thermodynamic data of $Cs_2Si_4O_9$(s) were obtained from Equations (46), (47), and (48). The data of TD for $Cs_2Si_4O_9$(s) are shown in Appendix B.

As mentioned above, the consistency and appropriateness of derived computational methodology were investigated by calculating the thermodynamic properties of $Cs_2Si_4O_9$[78]. Table 6 shows the comparison of the standard enthalpy of formation of $Cs_2Si_4O_9$ prototypes at 0 K derived from DFT calculations. As shown in this table, the P-3m1 configuration appears to be the most stable candidate for $Cs_2Si_4O_9$.

Then, vibrational properties, or phonon density of state (g(ω)), for the $Cs_2Si_4O_9$ candidates were examined, and their thermodynamic properties were determined. Table 7 shows the results of the calculated standard enthalpy and standard entropy for the $Cs_2Si_4O_9$ candidates together with the experimental values, and Figure 10 shows the results of the calculated and experimental heat capacities.

As shown in the abovementioned table and figure, the computed thermodynamic values for $Cs_2Si_4O_9$ were in good agreement with the experimental values, and the computational methodology used in this study was validated.

5.3.3. Solid iron-containing cesium silicate [$CsFeSiO_4$(s)]

There are no experimental values on the $CsFeSiO_4$ thermal properties in the literature. Thus, the same methodology as that used in the study on the thermodynamic properties of $Cs_2Si_4O_9$ (s) was applied to derive the thermodynamic properties of $CsFeSiO_4$(s) [78]. Table 8 shows the comparison of the standard enthalpy of formation of $CsFeSiO_4$ prototypes at 0 K derived from DFT calculations. As shown in this table, the $Pc2_1n$ configuration appears to be the most stable candidate for $CsFeSiO_4$.

Then, vibrational properties, or phonon density of state (g(ω)), for the $CsFeSiO_4$ candidates were examined, and their thermodynamic properties were determined. Table 9 shows the results of the calculated standard enthalpy and standard entropy for the $CsFeSiO_4$ candidates. Thus, the recommended values of the thermodynamic data of $CsFeSiO_4$ were obtained for the $Pc2_1n$ candidate and from the following equations[65,78]. The data of TD for $CsFeSiO_4$(s) is shown in Appendix B.

$$C_{\mathrm{p}}^{\circ}\ \mathrm{J/K/mol} = 133.6 + 0.08513(\mathrm{T/K}) - 4.316\times10^{-5}(\mathrm{T/K})^{2} - 2.025\times10^{6}(\mathrm{T/K})^{-2} \quad (49)$$

$$\Delta_{\mathrm{f}}H^{\circ}(298.15\ \mathrm{K}) = -1675\ \mathrm{kJ/mol} \quad (50)$$

$$S^{\circ}(298.15\ \mathrm{K}) = 177.9\ \mathrm{J\ /K/mol.} \quad (51)$$

Table 5 Computational parameters for k-mesh sampling and cutoff energy[65)]

(a) Parameters for $Cs_2Si_4O_9$ prototypes

Prototype	[$Na_2Ti_4O_9$] C2/m	[$K_2Ge_4O_9$] P–3c1	[Virtual] P 3-m1
E_{cut} (eV)	800	800	730
k-mesh	3×25×7	5×5×5	17×17×7
accuracy (meV/fu)	2	2	2

(b) Parameters for $CsFeSiO_4$ prototypes

Prototype	[$CsFeSiO_4$] $Pc2_1n$	[$KAlGeO_4$] $P6_3$	[$KAlSiO_4$] $P6_3$
E_{cut} (eV)	800	800	750
k-mesh	8×15×8	3×3×7	11×11×7
accuracy (meV/fu)	1	1	1

Table 6 Standard enthalpy of $Cs_2Si_4O_9$ prototypes at 0 K derived from DFT calculations[78)]

Prototype	$\Delta_f H_0°$ ($Cs_2Si_4O_9$)(kJ/mol)	δE(kJ/mol)*
[$Na_2Ti_4O_9$] C2/m	-3520	685
[$K_2Ge_4O_9$] P–3c1	-4154	51
[Virtual] P 3-m1	-4206	0

*δE is the difference with the lowest value

Table 7 Standard enthalpy of formation and standard entropy at 298 K compared with the experimental values[78)]

Prototype	$\Delta_f H_{298}°$ (kJ/mol)	$S_{298}°$ (J/K/mol)
[$K_2Ge_4O_9$] P–3c1	-4123	277.1
[Virtual] P 3-m1	-4178	302.7
Experimental value	-4297.6[76)]	322.1[77)]

Table 8 Standard enthalpy of $CsFeSiO_4$ prototypes at 0 K derived from DFT calculations[78)]

Prototype	$\Delta_f H_0°$($CsFeSiO_4$)(kJ/mol)	δE(kJ/mol)*
[$KAlSiO_4$] $P6_3$	-1659	9
[$KAlGeO_4$] $P6_3$	-1667	2
[$CsFeSiO_4$] $Pc2_1n$	-1669	0

*δE is the difference with the lowest value

Table 9 Standard enthalpy of formation and standard entropy at 298 K[78)]

Prototype	$\Delta_f H_{298}°$ (kJ/mol)	$S_{298}°$ (J/K/mol)
[$CsFeSiO_4$] $Pc2_1n$	-1657	177.9
[$KAlGeO_4$] $P6_3$	-1655	168.9

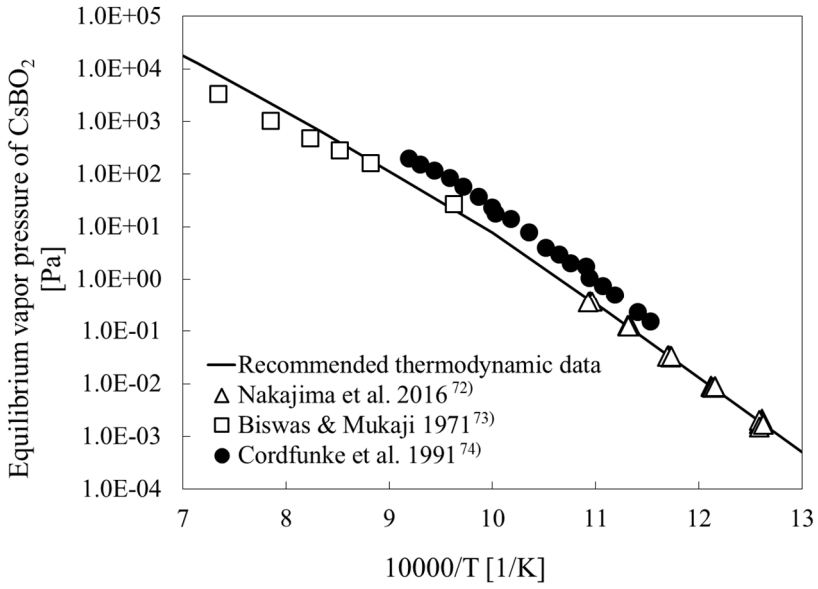

Figure 9 Comparison of equilibrium vapor pressures of $CsBO_2$[72,73,74)]

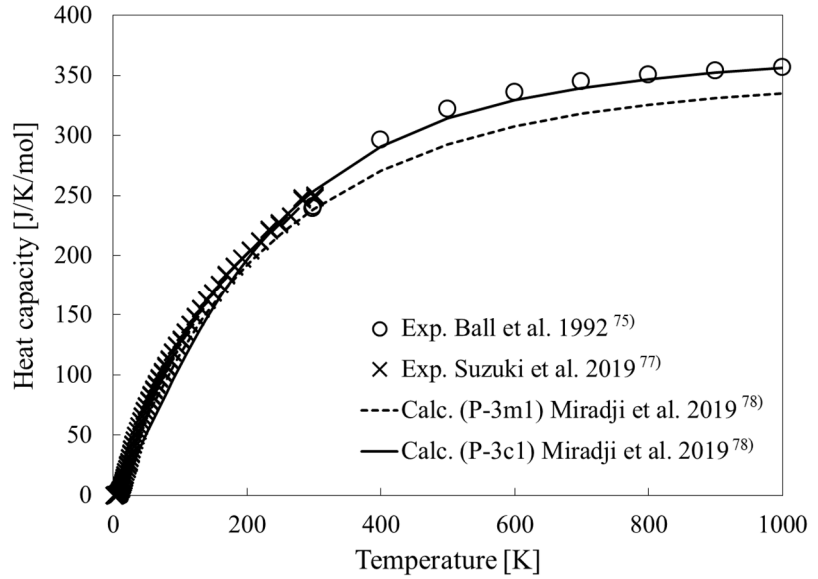

Figure 10 Comparison of heat capacities of $Cs_2Si_4O_9$ prototypes P-3m1[78)] and P-3c1[78)] with the experimental values[75,77)]

6. Conclusion

We integrated the FP chemistry datasets into the extended first version (version 1.1) of the FP chemistry database ECUME. ECUME is the database for the analysis of FP chemistry, which considerably affects all FP behaviors during an SA at a nuclear facility such as LWR. ECUME consists of three types of datasets: CRK, EM, and TD. This ECUME includes CRK for the reaction of Cs-I-B-Mo-O-H and Ru-N-O-H systems in the gas phase, EM for Cs chemisorption onto SS, and TD for $CsBO_2$ vapor and solid $Cs_2Si_4O_9$ and $CsFeSiO_4$. ECUME is the first database for the Cs-I-B-Mo-Fe-Si-O-H system in the world that is applicable for the evaluation of FP CRK.

Because in these SA analysis codes, the chemical forms of Cs were assumed to be CsI and CsOH, ECUME allows to analyze the chemical forms of Cs by considering the effects of B, Mo, Fe, and Si. Regarding the B effects, there is possibility that the lower volatile vapor species $CsBO_2$ is formed by the reaction between Cs vapor species and B vapor species at high temperature region during SA. It indicates that Cs may be retained as $CsBO_2$ in the higher temperature region in a reactor by the formation of aerosol and condensation onto a wall. On the other hand, the Cs vapor species and gaseous iodine species were transported toward the lower temperature region before reaching the chemical equilibrium. Even if this is the case, the appropriate chemical form of Cs can be estimated using ECUME CRK. Thus, ECUME provides more accurate Cs vapor species and gaseous iodine in the gas phase with B formed during BWR SA. Regarding the effects of Fe and Si, ECUME can reproduce the Cs chemisorption behavior onto SS more accurately, which allows to estimate the amount of compounds such as solid $Cs_2Si_4O_9$ and $CsFeSiO_4$. Thus, ECUME can contribute to the estimation of not only the amount of Cs under various chemical conditions, such as 1F, but also to the chemical properties of Cs deposits, which should be important for improved source term. The solubility and adherence of these Cs deposits is useful for estimating the dose change by the transportation of radioactive materials during the work caused by the decommissioning such as flooding by water.

Thus, the effects of B vapor as well as Fe, Si in SS on the Cs chemical behavior can be evaluated by applying ECUME to improve the current SA analysis code, which will result in a more reasonable evaluation of Cs distribution at 1F. ECUME provides the fundamental solution for the FP chemistry issues toward the 1F decommissioning work and the enhancement of LWR safety after the 1F SA.

References

[1] R.N. Morris, et al. :“Next Generation Nuclear Plant Phenomena Identification and Ranking Tables (PIRTs) Volume 3: Fission-Product Transport and Dose PIRTs”, NUREG/CR-6944, Vol. 3, (2007) (ORNL/TM-2007/147, Vol. 3).

[2] T. Haste, et al. :“SARNET integrated European Severe Accident Research – Conclusions in the source term area”, Nucl. Eng. Des., 239(12), pp.3116–3131 (2009).

[3] W. Klein-Heßling, et al. :“Conclusions on severe accident research priorities”, Ann. Nucl. Energy, 74, pp.4–11 (2014).

[4] S. Suehiro, et al. :“Development of the source term PIRT based on findings during Fukushima Daiichi NPPs accident”, Nucl. Eng. Des., 286, pp.163–174 (2015).

[5] Nuclear Damage Compensation and Decommissioning Facilitation Corporation :“Technical Strategic Plan 2017 for Decommissioning of the Fukushima Daiichi Nuclear Power Station of Tokyo Electric Power Company Holdings Inc.”, http://www.dd.ndf.go.jp/en/strategic-plan/index 2017.html, (accessed 22 Nov., 2019).

[6] R.O. Gauntt, et al. :“MELCOR Computer Code Manuals: Primer and User's Guide Version 1.8.5.”, NUREG/CR-6119 (2000).

[7] EPRI :“MAAP4, Modular Accident Analysis Program User’s Manual”, EPRI Report prepared by Fauske and Associates Inc. (1994).

[8] H. Ujita, et al. :“Development of Severe Accident Analysis Code SAMPSON in IMPACT Project”, J. Nucl. Sci. Technol., 36(11), pp.1076–1088 (1999).

[9] M. Kajimoto, et al. :“Development of THALES-2, a computer code for coupled thermal hydraulics and fission product transport analysis for severe accidents at LWRs and its application to analysis of fission product revapourization phenomena”, Int. Top. Mtg on Safety of Thermal Reactors, Portland, America (1991).

[10] IAEA :“Approaches and Tools for Severe Accident Analysis for Nuclear Power Plants”, Safety Report Series No. 56, 978-92-0-101608-9 (2008).

[11] L. Soffer, et al. :“Accident Source Terms for Light-Water Nuclear Power Plants”, NUREG-1465 (1995).

[12] B. Clément, et al. :“State of the Art Report on Iodine Chemistry”, OECD, NEA/CSNI/R(2007)1 (2007).

[13] H-J. Allelein, et al. :“State of the Art Report on Nuclear Aerosols”, OECD, NEA/CSNI/R(2009)5 (2009).

[14] S. Miwa, et al. :“Research Program for the Evaluation of Fission Product and Actinide Release Behaviour, Focusing on Their Chemical Forms”, Energy Procedia, 71, pp.168–181(2015).

[15] IRSN and CEA :“Research and development with regard to severe accidents in pressurised water reactors: Summary and outlook”, IRSN-2007/83, CEA-2007/351 (2007).

[16] M. Osaka, et al. :“Results and Progress of Fundamental Research on FP Chemistry”, Proc. The 8th European Review Meeting on Severe Accident Research – ERMSAR – 2017, Warsaw, Poland, 16–18 May, 2017.

[17] M. Osaka, et al. :“Results and progress of fundamental research on fission product chemistry; Progress report in 2015”, JAEA-Review 2016-026 (2016), 32p.

[18] N. Miyahara, et al. :“Chemical reaction kinetics dataset of Cs-I-B-Mo-O-H system for evaluation of fission product chemistry under LWR severe accident conditions”, J. Nucl. Sci. Technol., 56(2), pp.228–240 (2019).

[19] N. Miyahara, et al. :“Development of experimental and analytical technologies for fission product chemistry under LWR severe accident condition”, Proc. 2017 Water Reactor Fuel Performance Meeting, Jeju island, Korea, 10–14, Sep., 2017.

[20] S. Miwa, et al. :“Prediction of the effects of boron release kinetics on the vapor species of cesium and iodine fission products”, Prog. Nucl. Energy, 92, pp.254–259 (2016).

[21] K. Nakajima, et al. :“Termodynamic study of gaseous $CsBO_2$ by Knudsen effusion mass spectrometry”, J. Nucl. Mater., 491(1), pp.183–189 (2017).

[22] F.G. Di Lemma, et al. :“Surface analyses of cesium hydroxide chemisorbed onto type 304 stainless steel”, Nucl. Eng. Des., 305(15), pp.411–420 (2016).

[23] F.G. Di Lemma, et al. :“Experimental investigation of the influence of Mo contained in stainless steel on Cs chemisorption behavior”, J. Nucl. Mater., 484, pp.174–182 (2017).

[24] D.A. Powers, et al. :“A review of the technical issues of air ingression during severe reactor accidents”, NUREG/CR-6218 (1994).

[25] Y. Koma, et al. :“Radioactive contamination of several materials following the Fukushima Daiichi Nuclear Power Station accident”, Nucl. Mater. Energy, 10, pp.35–41 (2017).

[26] M. Kurata, et al. :“Thermodynamic evaluation on effect of sea water to degraded nuclear fuel in severe accident of LWR”, Transactions of the Atomic Energy Society of Japan, 12(4), pp.286–294 (2013).

[27] I. Sato, et al. :“Influence of boron vapor on transport behavior of deposited CsI during heating test simulating a BWR severe accident condition”, J. Nucl. Mater., 461, pp.22–28 (2015).

[28] B.R. Bowsher, et al. :“High Temperature Studies of Simulant Fission Products: Part III, Temperature-Dependent Interaction of Cesium Hydroxide Vapor with 304 Stainless Steel”, AEEW-R 1863 (1990).

[29] S.Y. Park, et al. :“Uncertainty Analysis of the Fission Product Behaviors during Severe Accidents for a Typical PWR”, Prog. Nucl. Sci. Technol., 1, pp.448–451 (2011).

[30] M. Ali, et al. :“Dust particle removal efficiency of a venturi scrubber”, Annals Nucl. Energ., 54,

pp.178–183 (2013).

[31] K.S. Lim, et al. :“Prediction for particle removal efficiency of a reverse jet scrubber”, J. Aerosol Sci., 37(12), pp.1826–1839 (2006).

[32] S. Calvert :“Venturi and other atomizing scrubbers efficiency and pressure drop”, AlChE J., 16 (3), pp.392–396 (1970).

[33] S.I. Pak, et al. :“Performance estimation of a venturi scrubber using a computational model for capturing dust particles with liquid spray”, J. Hazard. Mater., 138(3), pp.560–573 (2006).

[34] A.A. Noyes, et al. :“The rate of solution of solid substances in their own solutions”, J. Am. Chem. Soc., 19(12), pp.930–934 (1897).

[35] Y. Hattori, et al. :“Dissolution process analysis using model-free Noyes–Whitney integral equation”, Colloids and Surfaces B: Biointerfaces, 102(1), pp.227–231 (2013).

[36] L. Cantrel, et al. :“ASTEC V2 severe accident integral code: Fission product modelling and validation”, Nucl. Eng. Des., 272, pp.195–206 (2014).

[37] S. Miwa et al. :“Boron effects on fission product behavior under severe accident conditions”. Proc. Top Fuel 2016, Boise, America, 11–15 Sep., 2016.

[38] M. Valiev et al. :“NWChem: A comprehensive and scalable open-source solution for large scale molecular simulations”, Comput. Phys. Comm., 181(9), pp.1477–1489 (2010).

[39] N. González-García, et al. :“Searching for saddle points by using the nudged elastic band method: An implementation for gas-phase systems”, J. Chem. Theory Comput., 2(4), pp.895–904 (2006).

[40] O.K. Rice et al. :“Theories of unimolecular gas reactions at low pressures”, J. Am. Chem. Soc., 49(7), pp.1617–1629 (1927).

[41] L.S. Kassel :“Studies in homogeneous gas reactions. II. Introduction of quantum theory”, J. Phys. Chem., 32(7), pp.1065–1079 (1928).

[42] Thermo-Calc Software :“SSUB SGTE Substances Database version 6”, https://www.thermocalc.com/media/10097/ssub6.pdf, (accessed 22 Nov., 2019).

[43] J. McFarlane, et al. :“Chemical speciation of iodine source term to containment”, Nucl. Technol., 138(2), pp.162–178 (2002).

[44] A-C, Grégoire et al. :“Studies on the role of molybdenum on iodine transport in the RCS in nuclear severe accident conditions”, Ann. Nucl. Energy, 78, pp.117–129 (2015).

[45] R.O. Gauntt :“Synthesis of VERCORS and Phebus Data in Severe Accident Codes and Applications”, SAND2010-1633 (2010).

[46] F. Weigend et al. :“Balanced basis sets of split valence, triple zeta valence and quadruple zeta valence quality for H to Rn: Design and assessment of accuracy”, Phys. Chem. Chem. Phys., 7(18), pp.3297–3305 (2005).

[47] D. Rappoport et al. :“Property-optimized Gaussian basis sets for molecular response calculations”, J. Chem. Phys., 133(13), 134105 (2010).

[48] D. Andrae et al. :“Energy-adjusted *ab initio* pseudopotentials for the second and third row transition elements”, Theor. Chim. Acta., 77(2), pp.123–141 (1990).

[49] K.A. Peterson et al. :“Systematically convergent basis sets with relativistic pseudopotentials. II. Small-core pseudopotentials and correlation consistent basis sets for the post-d group 16-18 elements”, J. Chem. Phys., 119(21), 11113 (2003).

[50] T. Leininger, et al. :“The accuracy of the pseudopotential approximation: non-frozen-core effects for spectroscopic constants of alkali fluorides XF (X = K, Rb, Cs)”, Chem. Phys. Lett., 255(4–6), pp.274–280 (1996).

[51] Y. Zhao, et al. :“A new local density functional for main-group thermochemistry, transition metal bonding, thermochemical kinetics, and noncovalent interactions”, J. Chem. Phys., 125(19), 194101 (2006).

[52] G.C. Allen, et al. :“Surface studies of the interaction of cesium hydroxide vapor with 304 stainless steel”, Oxid. Met., 28 (1–2), pp.33–59 (1987).

[53] R.M. Elrick, et al. :“Reaction Between Some Cesium-Iodine Compounds and the Reactor Materials 304 Stainless Steel, Inconel 600 and Silver: Volume 1 Cesium Hydroxide Reactions” NUREG/CR-3197 vol. 1, SAND83-0395 (1984).

[54] S. Nishioka, et al. :“An experimental investigation of influencing chemical factors on Cs-chemisorption behavior onto stainless steel”, J. Nucl. Sci. Technol., 56(11), pp.988–995 (2019).

[55] K. Nakajima, et al. :“Study on chemisorption model of cesium hydroxide onto stainless steel type 304”, Proc. 27th International Conference on Nuclear Engineering, Ibaraki, Japan, 19-24 May, 2019.

[56] G. Kresse, et al. :“*Ab initio* molecular dynamics for liquid metals”, Phys. Rev. B, 47(1), pp.558–561 (1993).

[57] G. Kresse, et al. :“*Ab initio* molecular-dynamics simulation of the liquid-metal–amorphous-semiconductor transition in germanium”, Phys. Rev. B, 49, 14251 (1994).

[58] G. Kresse, et al. :“Efficiency of *ab-initio* total energy calculations for metals and semiconductors using a plane-wave basis set”, Comput. Mater. Sci., 6(1), pp.15–50 (1996).

[59] G. Kresse, et al. :“Efficient iterative schemes for *ab initio* total-energy calculations using a plane-wave basis set”, Phys. Rev. B, 54, 11169 (1996).

[60] D. Vanderbilt :“Soft self-consistent pseudopotentials in a generalized eigenvalue formalism”, Phys. Rev. B, 41, 7892 (1990).

[61] G. Kresse, et al. :“Norm-conserving and ultrasoft pseudopotentials for first-row and transition elements”, J. Phys: Condensed Matter, 6(40), pp.8245–8257 (1994).

[62] J.P. Perdew, et al. :“Generalized Gradient Approximation Made Simple”, Phys. Rev. Lett., 77(18), pp.3865–3868 (1996).

[63] N.J. Mosey, et al. :“Rotationally invariant *ab initio* evaluation of Coulomb and exchange

parameters for DFT+U calculations", J. Chem. Phys., 129(1), 14103 (2008).

[64] V. Stevanovi´c, et al. :"Correcting density functional theory for accurate predictions of compound enthalpies of formation: Fitted elemental-phase reference energies", Phys. Rev. B, 85, 115104 (2012).

[65] F. Miradji, et al. :"Modelling of cesium chemisorption under nuclear power plant severe accident conditions", The 9th European Review Meeting on Severe Accident Research – ERMSAR – 2019, Prague, Czech Republic, 18–20 Mar., 2019.

[66] K. Momma, et al. :"VESTA3 for three-dimensional visualization of crystal, volumetric and morphology data", J. App. Cryst., 44 (6), pp.1272–1276 (2011).

[67] A. Togo, et al. :"First principles phonon calculations in materials science", Scr. Mater., 108, pp.1–5 (2015).

[68] M.W. Chase, et al. :"NIST-JANAF thermochemical tables fourth edition, Part I, Al – Co", J. Phys. Chem. Ref. Data, Monograph, No. 9, pp.15–16 (1998).

[69] E.H.P. Cordfunke, et al. (Eds.) :"Thermochemical Data for Reactor Materials and Fission Products", North Holland, 978-04-4-488485-5, pp.131–134 (1990).

[70] Yu.S. Ezhov, et al. :"Electron diffraction study of the molecular structure of cesium metaborate", J. Struct. Chem., 41(1), pp.55–60 (2000).

[71] K. Nakajima, et al. :"Thermodynamic study of gaseous $CsBO_2$ by Knudsen effusion mass spectrometry", J. Nucl. Mater., 491(1), pp.183–189 (2017).

[72] K. Nakajima, :"Determination of optimal vapor pressure data by the second and third law methods", Mass Spectrom., 5(2), S0055 (2016).

[73] S.R. Biswas, et al. :"Vapor pressure of cesium metaborate", J. Chem. Eng. Data, 16(3), pp.336–337 (1971).

[74] E.H.P. Cordfunke, et al. :"Vapour pressures of some caesium compounds I. $CsBO_2$", J. Chem. Thermodyn., 23(3), pp.297–300 (1991).

[75] R.G.J. Ball, et al. :"Thermochemical data acquisition – Part II", EUR 14844 EN (1992).

[76] E.H.P. Cordfunke, et al. :"The standard molar enthalpies of formation of Cs_2MnO_4, $Cs_2Si_4O_9$ and Cs_3PO_4", J. Chem. Thermodyn., 25(8), pp.1011–1016 (1993).

[77] E. Suzuki, et al. :"FP chemistry in a high temperature region of LWR under a severe accident (4) Thermodynamic property of cesium-silicates", Annual meeting of Atomic Energy Society of Japan 2018, 2D18, 26–28, Mar., 2018.

[78] F. Miradji, et al. :"Cesium chemisorbed species onto stainless steel surfaces: an atomistic scale study", J. Phy. Chem. Solid., 136, 109168 (2020).

[79] L. Cantrel, et al. :"Advances in mechanistic understanding of iodine behavior in PHEBUS-FP tests with the help of *ab initio* calculations", Ann. Nucl. Energy, 61, pp.170–178 (2013).

[80] Y. Zhao, et al. :"A new local density functional for main-group thermochemistry, transition metal

bonding, thermochemical kinetics, and noncovalent interactions". J. Chem. Phys., 125(19), 194101 (2006).

[81] S. Canneaux, et al. :"Theoretical study of the gas-phase reactions of iodine atoms ($^2P_{3/2}$) with H_2, H_2O, HI, and OH", J. Phys. Chem. A., 114, pp.9270–9288 (2010).

[82] C. Hammaecher, et al. :"A theoretical study of the H-abstraction reactions from HOI by moist air radiolytic products (H, OH, and O (^3P)) and iodine atoms ($^2P_{3/2}$)", J. Phys. Chem. A., 115(24), pp.6664–6674 (2011).

[83] B. Xerri, et al. :"*Ab initio* calculations and iodine kinetic modeling in the reactor coolant system of a pressurized water reactor in case of severe nuclear accident", Comput. Theor. Chem., 990(15), pp.194–208 (2012).

[84] L. Cantrel, et al. :"Reaction kinetics of a fission-product mixture in a steam-hydrogen carrier gas in the Phebus primary circuit", Nucl. Technol., 144(1), pp.1–15 (2003).

[85] R. Atkinson, et al. :"Evaluated kinetic and photochemical data for atmospheric chemistry: Volume III - gas phase reactions of inorganic halogens", Atmos. Chem. Phys., 7, pp.981–1191(2007).

[86] D.L. Baulch, et al. :"Evaluated kinetic data for combustion modelling", J. Phys. Chem. Ref. Data, 21(3), pp.411–429 (1992).

[87] D.L. Baulch, et al. :"Evaluated kinetic data for combustion modelling Supplement I". J. Phys. Chem. Ref. Data., 23, pp.847–1033 (1994).

[88] R.C. Brown, et al. :"Gas phase kinetic modeling and sensitivity analysis of B/H/O/C/F combustion systems", US: Office of Naval Research; ARI-RR-964 (1993).

[89] L. Pasternack, et al. :"Gas-phase modeling of homogeneous boron / oxygen / hydrogen / carbon combustion", Comb. Flame, 90, pp.259–268 (1992).

[90] D.P. Chakraborty, et al. :"Theoretical study of the OH + NO_2 reaction: formation of nitric acid and the hydroperoxyl radical", Chem. Phys., 231(1), pp.39–49 (1998).

[91] D.L. Baulch, et al. :"Evaluated kinetic data for combustion modeling: Supplement II", J. Phys. Chem. Ref. Data, 34(3), pp.757–1397 (2005).

[92] H.S. Johnston, et al. :"Unimolecular decomposition of NO_3 to form NO and O_2 and a review of N_2O_5/NO_3 kinetics", J. Geophysical Research, 91, pp.5159–5172 (1986).

[93] W.C. Jr. Gardiner (Eds.) :"Gas-phase combustion chemistry", Springer-Verlag New York, 978-1-4612-1310-9, (2000).

[94] W. Tsang et al. :"Chemical kinetic data base for propellant combustion I. Reactions involving NO, NO_2, HNO, HNO_2, HCN and N_2O", J. Phys. Chem. Ref. Data, 20 (4), pp.609–663 (1991).

[95] M.-C. Su, et al. :"Rate Constants, $1100 \leq T \leq 2000$ K, for H + $NO_2 \rightarrow$ OH + NO Using Two Shock Tube Techniques: Comparison of Theory to Experiment", J. Phys. Chem. A, 106(36), pp.8261–8270 (2002).

[96] M. Abian, et al. :"Formation of NO from N_2/O_2 mixtures in a flow reactor: Toward an accurate

prediction of thermal NO", Int. J. Chem, Kinet., 47(8), pp.518–532 (2015).

[97] R. Atkinson, et al. :"Evaluated kinetic and photochemical data for atmospheric chemistry: Volume I – gas phase reactions of O_x, HO_x, NO_x and SO_x species", Atmos. Chem. Phys., 4(6), pp.1461–1738 (2004).

[98] W.S. Xia, et al. :"A multifacet mechanism for the OH + HNO_3 reaction: An *ab initio* molecular orbital/statistical theory study", J. Chem. Phys., 114(10), pp.4522–4532 (2001).

Appendix

A) Dataset for chemical reaction kinetics (CRK)

a. Dataset of chemical reaction rate constants *k* for Cs-I-B-Mo-O-H system

$$k = AT^n \exp\left(-\frac{E}{\mathrm{R}T}\right)$$

Chemical reactions	A [a] (cm^3/mol-s)	n	E (J/mol)	Ref.
$I + H_2 \rightarrow HI + H$	2.4×10^{8}	1.93	1.28×10^{5}	[79]
$I + H_2O \rightarrow HI + OH$	3.1×10^{7}	2.26	1.81×10^{5}	[79]
$I + HI \rightarrow H + I_2$	5.8×10^{8}	1.72	1.49×10^{5}	[80]
$I + OH \rightarrow HI + O$	2.8×10^{8}	1.70	1.24×10^{5}	[79]
$H_2 + IO \rightarrow HOI + H$	6.6×10^{-1}	4.00	4.38×10^{4}	[81]
$I + HOI \rightarrow HI + IO$	2.3×10^{6}	2.29	1.11×10^{5}	[81]
$OH + IO \rightarrow HOI + O$	5.7×10^{-5}	4.93	1.70×10^{4}	[81]
$OH + HOI \rightarrow IO + H_2O$	4.3×10^{-3}	4.33	-1.90×10^{4}	[81]
$I + HO_2 \rightarrow HI + O_2$	9.0×10^{12}	0.00	9.06×10^{3}	[79]
$HO_2 + IO \rightarrow HOI + O_2$	8.4×10^{12}	0.00	-4.49×10^{3}	[79]
$O + I_2 \rightarrow I + IO$	7.5×10^{13}	0.00	0.00	[79]
$I_2 + H_2 \rightarrow HI + HI$	1.9×10^{14}	0.00	1.71×10^{5}	[79]
$O + IO \rightarrow I + O_2$	8.4×10^{13}	0.00	0.00	[82]
$HOI + H \rightarrow I + H_2O$	6.0×10^{8}	1.55	1.05×10^{4}	[79]
$I_2 + OH \rightarrow HOI + I$	1.2×10^{7}	1.90	-1.20×10^{4}	[79]
$OH + HI \rightarrow HOI + H$	8.4×10^{5}	2.28	9.33×10^{4}	[83]
$OH + I \rightarrow IO + H$	1.5×10^{14}	0.00	2.68×10^{5}	[79]
$HO_2 + I \rightarrow OH + IO$	3.8×10^{13}	0.00	4.74×10^{3}	[79]
$I + I + M \rightarrow I_2 + M$	2.4×10^{14}	0.00	-6.27×10^{3}	[79]
$I + H + M \rightarrow HI + M$	2.0×10^{21}	-1.87	0.00	[79]
$I + OH + M \rightarrow HOI + M$	1.0×10^{15}	0.00	0.00	[79]
$HOI + HI \rightarrow I_2 + H_2O$	2.2×10^{5}	0.43	1.41×10^{5}	[84]
$Cs + HI \rightarrow CsI + H$	9.3×10^{9}	1.56	-1.11×10^{4}	[85]
$CsI (+ M) \rightarrow Cs + I (+ M)$ [b]	1.4×10^{13}	0.00	3.35×10^{5}	[84]
$CsI + CsI (+M) \rightarrow Cs_2I_2 (+M)$ [b]	3.2×10^{6}	1.14	1.71×10^{5}	[84]
$Cs + H_2O \rightarrow CsOH + H$	1.3×10^{11}	0.58	1.34×10^{5}	[84]
$CsOH + HI \rightarrow CsI + H_2O$	9.8×10^{8}	-0.41	1.19×10^{5}	[84]

Chemical reactions	A [a] (cm^3/mol-s)	n	E (J/mol)	Ref.
CsI + OH → I + CsOH	1.0×10^{14}	1.00	0.00	[18]
IO + HI → I_2 + OH	1.0×10^{10}	0.68	2.56×10^{5}	[18]
I_2 + CsOH → HOI + CsI	1.4×10^{14}	1.00	0.00	[18]
IO + H → O + HI	1.1×10^{17}	-1.57	1.75×10^{4}	[18]
IO + H_2 → OH + HI	5.7×10^{2}	3.27	9.07×10^{4}	[18]
IO+ OH → O_2 + HI	1.6×10^{9}	0.99	2.89×10^{5}	[18]
HOI + O → O_2 + HI	2.0×10^{12}	0.14	2.39×10^{5}	[18]
HOI + H_2 → HI + H_2O	9.6×10^{7}	1.18	1.83×10^{5}	[18]
IO + Cs → O + CsI	2.2×10^{14}	1.00	0.00	[18]
I +O + M → IO + M	1.1×10^{17}	2.00	0.00	[18]
CsOH + CsOH + M → $Cs_2O_2H_2$ + M	1.4×10^{16}	2.00	0.00	[18]
IO + IO → O_2 + I_2	1.5×10^{4}	2.41	1.72×10^{6}	[18]
HOI + Cs → OH + CsI	2.2×10^{14}	1.00	4.19×10^{4}	[18]
HI + O + M → HOI + M	1.2×10^{17}	2.00	0.00	[18]
HOI + Cs → I + CsOH	2.2×10^{14}	1.00	0.00	[18]
Cs + OH + M → CsOH + M	6.0×10^{16}	2.00	0.00	[18]
I_2 + Cs → I + CsI	1.7×10^{14}	1.00	0.00	[18]
IO + H + M → HOI + M	1.2×10^{17}	2.00	0.00	[18]
IO + H_2 → I + H_2O	2.0×10^{11}	0.66	3.22×10^{5}	[18]
OH + OH → H_2O + O	1.5×10^{9}	1.14	4.20×10^{2}	[79]
OH + H_2 → H_2O + H	1.8×10^{9}	1.21	1.97×10^{4}	[79]
O + H_2 → OH + H	5.1×10^{4}	2.67	2.63×10^{4}	[79]
O + OH → O_2 + H	2.8×10^{11}	0.40	-3.09×10^{3}	[79]
H_2O + M → H + OH + M	1.3×10^{15}	0.00	4.40×10^{5}	[86]
OH + M → O + H + M	2.4×10^{15}	0.00	4.16×10^{5}	[79]
HO_2 + H → H_2 + O_2	6.7×10^{7}	1.77	-2.38×10^{3}	[79]
HO_2 + H → H_2O + O	9.1×10^{8}	1.47	5.81×10^{4}	[79]
HO_2 + H → OH + OH	2.2×10^{11}	0.88	-2.70×10^{2}	[79]
HO_2 + OH → H_2O + O_2	2.9×10^{13}	0.00	-2.08×10^{3}	[79]
H_2 + M → H + H + M	2.2×10^{14}	0.00	4.02×10^{5}	[87]

Chemical reactions	A [a] (cm^3/mol-s)	n	E (J/mol)	Ref.
$O_2 + M \rightarrow O + O + M$	1.8×10^{18}	-1.00	4.94×10^{5}	[79]
$H + O_2 + M \rightarrow HO_2 + M$	6.2×10^{17}	-0.80	0.00	[87]
$HO_2 + O \rightarrow OH + O_2$	3.2×10^{13}	0.00	0.00	[87]
$HO_2 + HO_2 \rightarrow H_2O_2 + O_2$	4.2×10^{14}	0.00	5.01×10^{4}	[87]
$H_2O_2 + M \rightarrow OH + OH + M$	1.8×10^{16}	0.00	1.80×10^{5}	[87]
$H_2O_2 + H \rightarrow H_2O + OH$	1.0×10^{13}	0.00	1.50×10^{4}	[87]
$H_2O_2 + H \rightarrow H_2 + HO_2$	1.7×10^{12}	0.00	1.57×10^{4}	[87]
$H_2O_2 + O \rightarrow HO_2 + OH$	6.6×10^{11}	0.00	1.66×10^{4}	[87]
$H_2O_2 + OH \rightarrow HO_2 + H_2O$	7.8×10^{12}	0.00	5.57×10^{3}	[87]
$OH + OH \rightarrow O_2 + H_2$	2.0×10^{13}	-1.30	2.29×10^{5}	[84]
$B + O_2 \rightarrow BO + O$	7.2×10^{13}	0.00	1.30×10^{3}	[88]
$B + O + M \rightarrow BO + M$	1.1×10^{15}	-0.50	-8.33×10^{3}	[88]
$BO + O_2 \rightarrow BO_2 + O$	4.2×10^{12}	0.00	-2.13×10^{3}	[88]
$BO + O + M \rightarrow BO_2 + M$	1.1×10^{15}	0.00	-8.33×10^{3}	[88]
$B + BO_2 \rightarrow BO + BO$	3.6×10^{13}	0.00	0.00	[88]
$BO + BO_2 + M \rightarrow B_2O_3 + M$	1.8×10^{13}	0.00	-8.33×10^{3}	[88]
$BO_2 + BO_2 \rightarrow B_2O_3 + O$	6.0×10^{10}	0.00	4.16×10^{4}	[88]
$B + OH \rightarrow BO + H$	6.0×10^{13}	0.00	0.00	[88]
$BO + OH \rightarrow BO_2 + H$	2.4×10^{12}	0.00	0.00	[88]
$BO + OH + M \rightarrow HBO_2 + M$	3.6×10^{14}	0.00	-8.33×10^{3}	[88]
$BO + H_2O \rightarrow HBO_2 + H$	6.0×10^{10}	0.00	4.16×10^{4}	[89]
$BO_2 + OH \rightarrow HBO_2 + O$	1.8×10^{12}	0.00	4.14×10^{3}	[88]
$BO_2 + H + M \rightarrow HBO_2 + M$	1.8×10^{15}	0.00	-8.33×10^{3}	[88]
$BO_2 + H_2 \rightarrow HBO_2 + H$	1.8×10^{12}	0.00	8.33×10^{3}	[88]
$HBO_2 + OH \rightarrow BO_2 + H_2O$	1.2×10^{12}	0.00	8.33×10^{3}	[88]
$B_2O_3 + H_2O \rightarrow HBO_2 + HBO_2$	6.0×10^{8}	0.00	4.99×10^{4}	[88]
$BO + H + M \rightarrow HBO + M$	1.1×10^{15}	0.00	-8.33×10^{3}	[88]
$BO + H_2 \rightarrow HBO + H$	4.5×10^{1}	3.53	1.32×10^{4}	[88]
$BO + OH \rightarrow HBO + O$	1.6×10^{3}	2.76	2.10×10^{4}	[88]
$HBO + O \rightarrow BO_2 + H$	4.8×10^{13}	0.00	2.10×10^{4}	[88]

Chemical reactions	A [a] (cm^3/mol-s)	n	E (J/mol)	Ref.
$HBO + OH \rightarrow BO + H_2O$	4.8×10^{13}	0.00	0.00	[88]
$HBO + OH \rightarrow HBO_2 + H$	4.8×10^{13}	0.00	0.00	[88]
$HBO + OH \rightarrow BO_2 + H_2$	6.0×10^{3}	0.00	2.93×10^{5}	[88]
$HBO + O_2 \rightarrow BO_2 + OH$	6.0×10^{3}	0.00	2.93×10^{5}	[88]
$HBO + O + M \rightarrow HBO_2 + M$	3.6×10^{20}	0.00	2.09×10^{5}	[88]
$BO + BO + M \rightarrow B_2O_2 + M$	3.6×10^{13}	0.00	-8.33×10^{3}	[88]
$B_2O_2 + H \rightarrow HBO + BO$	6.0×10^{13}	0.00	0.00	[88]
$B_2O_2 + O \rightarrow BO + BO_2$	3.6×10^{13}	0.00	0.00	[88]
$B_2O_2 + OH \rightarrow BO + HBO_2$	3.6×10^{3}	0.00	0.00	[88]
$B_2O_2 + OH \rightarrow BO_2 + HBO$	6.0×10^{3}	0.00	2.93×10^{5}	[88]
$B_2O_2 + O_2 \rightarrow BO_2 + BO_2$	6.0×10^{3}	0.00	3.35×10^{5}	[88]
$B + H_2O \rightarrow HBO + H$	2.4×10^{14}	0.00	1.12×10^{4}	[88]
$HBO + BO_2 \rightarrow HBO_2 + BO$	1.8×10^{12}	0.00	4.14×10^{3}	[88]
$HBO + BO_2 \rightarrow B_2O_3 + H$	1.8×10^{12}	0.00	4.14×10^{3}	[88]
$HBO_2 + BO \rightarrow B_2O_3 + H$	4.8×10^{12}	0.00	0.00	[88]
$B + H + M \rightarrow BH + M$	1.1×10^{15}	0.00	-8.33×10^{3}	[89]
$B + H_2 + M \rightarrow BH_2 + M$	1.1×10^{11}	0.00	0.00	[89]
$B + H_2O \rightarrow BOH + H$	4.8×10^{12}	0.00	0.00	[89]
$B + OH + M \rightarrow BOH + M$	1.1×10^{15}	0.00	-8.33×10^{3}	[89]
$BH + O \rightarrow BO + H$	1.0×10^{13}	0.00	0.00	[89]
$BH + O_2 \rightarrow HBO + O$	3.0×10^{13}	0.00	1.00×10^{4}	[89]
$BH + H_2O \rightarrow HBO + H_2$	3.0×10^{12}	0.00	1.59×10^{3}	[89]
$BH + O + M \rightarrow HBO + M$	1.1×10^{15}	0.00	-8.33×10^{3}	[89]
$BH + OH \rightarrow HBO + H$	3.0×10^{13}	0.00	1.00×10^{4}	[89]
$BH + BO_2 \rightarrow HBO + BO$	9.0×10^{11}	0.00	1.00×10^{4}	[89]
$BH + BO \rightarrow HBO + B$	9.0×10^{11}	0.00	1.00×10^{4}	[89]
$BH + HBO_2 \rightarrow HBO + HBO$	3.0×10^{12}	0.00	1.59×10^{3}	[89]
$BH_2 + BO \rightarrow HBO + BH$	6.0×10^{11}	0.00	0.00	[89]
$BH_2 + O \rightarrow HBO + H$	1.0×10^{13}	0.00	0.00	[89]
$BH_2 + O \rightarrow BH + OH$	1.0×10^{13}	0.00	0.00	[89]

Chemical reactions	A [a] (cm^3/mol-s)	n	E (J/mol)	Ref.
$BH_2 + OH \rightarrow BH + H_2O$	5.0×10^{12}	0.00	0.00	[89]
$HBO + O_2 \rightarrow HBO_2 + O$	4.8×10^{10}	0.00	0.00	[89]
$HBO + H_2O \rightarrow HBO_2 + H_2$	4.8×10^{10}	0.00	0.00	[89]
$HBO + HO_2 \rightarrow HBO_2 + OH$	4.8×10^{10}	0.00	0.00	[89]
$BO + H_2 \rightarrow BOH + H$	4.5×10^{1}	3.53	1.32×10^{4}	[89]
$BOH + M \rightarrow HBO + M$	3.6×10^{13}	0.00	9.79×10^{4}	[89]
$BOH + BO_2 \rightarrow HBO_2 + BO$	4.2×10^{12}	0.00	-2.12×10^{3}	[89]
$BOH + O_2 \rightarrow HBO_2 + O$	4.2×10^{12}	0.00	-2.12×10^{3}	[89]
$BOH + OH \rightarrow HBO_2 + H$	2.4×10^{12}	0.00	0.00	[89]
$BOH + H_2O \rightarrow HBO_2 + H_2$	6.0×10^{10}	0.00	4.16×10^{4}	[89]
$BOH + O + M \rightarrow HBO_2 + M$	1.1×10^{15}	0.00	-8.33×10^{3}	[89]
$BOH + O \rightarrow BO_2 + H$	4.8×10^{13}	0.00	0.00	[89]
$BOH + HBO_2 \rightarrow B_2O_3 + H_2$	4.8×10^{10}	0.00	0.00	[89]
$BOH + OH \rightarrow BO + H_2O$	4.8×10^{13}	0.00	0.00	[89]
$BOH + O \rightarrow BO + OH$	4.8×10^{13}	0.00	0.00	[89]
$BO_2 + BH \rightarrow HBO_2 + B$	1.8×10^{12}	0.00	4.14×10^{3}	[89]
$BO_2 + BH_2 \rightarrow HBO_2 + BH$	1.8×10^{12}	0.00	4.14×10^{3}	[89]
$HBO_2 + HBO \rightarrow B_2O_3 + H_2$	4.8×10^{10}	0.00	0.00	[89]
$B_2O_2 + H \rightarrow BOH + BO$	3.6×10^{13}	0.00	0.00	[89]
$B_2O_2 + OH \rightarrow B_2O_3 + H$	6.0×10^{11}	0.00	0.00	[89]
$B_2O_2 + H_2O \rightarrow B_2O_3 + H_2$	6.0×10^{10}	0.00	0.00	[89]
$B_2O_2 + BO_2 \rightarrow B_2O_3 + BO$	6.0×10^{12}	0.00	0.00	[89]
$BO + H_3BO_3 \rightarrow HBO_2 + H_2BO_2$	2.4×10^{5}	2.23	8.51×10^{4}	[18]
$H_2BO_2 + H_2O \rightarrow H_3BO_3 + H$	3.1×10^{8}	0.71	5.35×10^{4}	[18]
$B + H_3BO_3 \rightarrow BOH + H_2BO_2$	1.3×10^{12}	1.01	2.62×10^{4}	[18]
$H_2BO_2 + H_2BO_2 \rightarrow BOH + H_3BO_3$	1.3×10^{3}	1.96	0.00	[18]
$HBO_2 + H_2O + M \rightarrow H_3BO_3 + M$	8.8×10^{16}	2.00	0.00	[18]
$B + H_3BO_3 \rightarrow HBO + H_2BO_2$	2.9×10^{14}	1.00	0.00	[18]
$H_2BO_2 + H_2BO_2 \rightarrow HBO + H_3BO_3$	3.2×10^{0}	2.92	0.00	[18]
$H_2BO_2 + OH + M \rightarrow H_3BO_3 + M$	8.8×10^{16}	2.00	0.00	[18]

Chemical reactions	A [a] (cm^3/mol-s)	n	E (J/mol)	Ref.
$CsBO_2 + H \rightarrow HBO_2 + Cs$	1.2×10^{14}	1.00	0.00	[18]
$BO + CsBO_2 \rightarrow B_2O_3 + Cs$	1.9×10^{14}	1.00	0.00	[18]
$B + CsBO_2 \rightarrow B_2O_2 + Cs$	1.5×10^{14}	1.00	0.00	[18]
$BO_2 + Cs + M \rightarrow CsBO_2 + M$	2.2×10^{16}	2.00	0.00	[18]
$H_2BO_2 + Cs \rightarrow CsBO_2 + H_2$	3.4×10^{17}	-0.73	2.49×10^{4}	[18]
$Mo + O + M \rightarrow MoO + M$	2.1×10^{17}	2.00	0.00	[18]
$MoO + O + M \rightarrow MoO_2 + M$	5.7×10^{16}	2.00	0.00	[18]
$MoO_2 + O + M \rightarrow MoO_3 + M$	4.5×10^{16}	2.00	0.00	[18]
$MoO_3 + O + M \rightarrow MoO_4 + M$	2.9×10^{16}	2.00	0.00	[18]
$Mo + O_2 \rightarrow MoO + O$	2.6×10^{15}	1.00	0.00	[18]
$MoO + O_2 \rightarrow MoO_2 + O$	7.0×10^{14}	1.00	0.00	[18]
$MoO_2 + O_2 \rightarrow MoO_3 + O$	5.5×10^{14}	1.00	0.00	[18]
$MoO_3 + O_2 \rightarrow MoO_4 + O$	4.5×10^{15}	1.00	8.10×10^{5}	[18]
$Mo + H_2O \rightarrow MoO + H_2$	2.6×10^{15}	1.00	0.00	[18]
$MoO + H_2O \rightarrow MoO_2 + H_2$	7.0×10^{14}	1.00	0.00	[18]
$MoO_2 + H_2O \rightarrow MoO_3 + H_2$	5.5×10^{14}	1.00	0.00	[18]
$MoO_3 + H_2O \rightarrow MoO_4 + H_2$	4.0×10^{15}	1.00	7.63×10^{5}	[18]
$Mo + OH \rightarrow MoO + H$	2.6×10^{15}	1.00	0.00	[18]
$MoO + OH \rightarrow MoO_2 + H$	7.0×10^{14}	1.00	0.00	[18]
$MoO_2 + OH \rightarrow MoO_3 + H$	5.5×10^{14}	1.00	0.00	[18]
$MoO_3 + OH \rightarrow MoO_4 + H$	9.3×10^{15}	1.00	7.08×10^{5}	[18]
$MoO_3 + MoO_3 + M \rightarrow Mo_2O_6 + M$	2.2×10^{16}	2.00	0.00	[18]
$MoO_3 + CsOH \rightarrow CsMoO_4 + H$	1.3×10^{14}	1.00	0.00	[18]
$MoO_4 + Cs + M \rightarrow CsMoO_4 + M$	1.6×10^{16}	2.00	0.00	[18]
$MoO_4 + CsOH \rightarrow CsMoO_4 + OH$	1.8×10^{14}	1.00	0.00	[18]
$MoO_4 + CsI \rightarrow CsMoO_4 + I$	1.9×10^{14}	1.00	0.00	[18]
$MoO_4 + CsBO_2 \rightarrow CsMoO_4 + BO_2$	1.9×10^{14}	1.00	0.00	[18]
$CsMoO_4 + Cs + M \rightarrow Cs_2MoO_4 + M$	5.5×10^{15}	2.00	0.00	[18]
$CsMoO_4 + CsOH \rightarrow Cs_2MoO_4 + OH$	4.4×10^{13}	1.00	0.00	[18]
$CsMoO_4 + CsI \rightarrow Cs_2MoO_4 + I$	6.7×10^{13}	1.00	0.00	[18]

Chemical reactions	A [a] (cm^3/mol-s)	n	E (J/mol)	Ref.
$CsMoO_4 + CsBO_2 \rightarrow Cs_2MoO_4 + BO_2$	1.2×10^{14}	1.00	6.43×10^{3}	[18]
$Mo + I + M \rightarrow MoI + M$	3.9×10^{16}	2.00	0.00	[18]
$MoI + I + M \rightarrow MoI_2 + M$	1.5×10^{16}	2.00	0.00	[18]
$MoI_2 + I + M \rightarrow MoI_3 + M$	9.1×10^{15}	2.00	0.00	[18]
$MoI_3 + I + M \rightarrow MoI_4 + M$	9.8×10^{15}	2.00	0.00	[18]
$Mo + I_2 \rightarrow MoI + I$	2.3×10^{14}	1.00	0.00	[18]
$MoI + I_2 \rightarrow MoI_2 + I$	1.1×10^{14}	1.00	2.22×10^{5}	[18]
$MoI_2 + I_2 \rightarrow MoI_3 + I$	1.2×10^{14}	1.00	0.00	[18]
$MoI_3 + I_2 \rightarrow MoI_4 + I$	1.2×10^{14}	1.00	0.00	[18]
$Mo + HI \rightarrow MoI + H$	4.8×10^{14}	1.00	0.00	[18]
$MoI + HI \rightarrow MoI_2 + H$	5.8×10^{15}	1.00	3.76×10^{5}	[18]
$MoI_2 + HI \rightarrow MoI_3 + H$	1.1×10^{14}	1.00	0.00	[18]
$MoI_3 + HI \rightarrow MoI_4 + H$	5.8×10^{15}	1.00	1.16×10^{5}	[18]
$Mo + CsI \rightarrow MoI + Cs$	1.4×10^{14}	1.00	4.38×10^{4}	[18]
$MoI + CsI \rightarrow MoI_2 + Cs$	1.1×10^{14}	1.00	4.28×10^{5}	[18]
$MoI_2 + CsI \rightarrow MoI_3 + Cs$	4.3×10^{13}	1.00	0.00	[18]
$MoI_3 + CsI \rightarrow MoI_4 + Cs$	1.2×10^{14}	1.00	0.00	[18]
$Mo + IO \rightarrow MoI + O$	6.5×10^{13}	1.00	0.00	[18]
$MoI + IO \rightarrow MoI_2 + O$	1.5×10^{15}	1.00	2.51×10^{5}	[18]
$MoI_2 + IO \rightarrow MoI_3 + O$	1.0×10^{14}	1.00	0.00	[18]
$MoI_3 + IO \rightarrow MoI_4 + O$	1.7×10^{9}	0.44	3.67×10^{3}	[18]
$Mo + HOI \rightarrow MoI + OH$	2.1×10^{13}	1.00	0.00	[18]
$MoI + HOI \rightarrow MoI_2 + OH$	1.5×10^{15}	1.00	2.65×10^{5}	[18]
$MoI_2 + HOI \rightarrow MoI_3 + OH$	1.1×10^{14}	1.00	0.00	[18]
$MoI_3 + HOI \rightarrow MoI_4 + OH$	1.5×10^{15}	1.00	4.34×10^{3}	[18]

Chemical reactions	A [a] (cm^3/mol-s)	n	E (J/mol)	Ref.
$BO + CsOH \rightarrow H + CsBO_2$	1.7×10^{14}	1.00	0.00	
$BO_2 + CsOH \rightarrow OH + CsBO_2$	1.8×10^{14}	1.00	0.00	
$BO_2 + CsI \rightarrow I + CsBO_2$	1.7×10^{14}	1.00	0.00	
$B_2O_3 + CsOH \rightarrow HBO_2 + CsBO_2$	1.2×10^{14}	1.00	0.00	
$HBO_2 + CsOH \rightarrow H_2O + CsBO_2$	1.7×10^{14}	1.00	0.00	
$HBO_2 + CsI \rightarrow HI + CsBO_2$	1.3×10^{14}	1.00	7.83×10^{4}	
$BOH + CsOH \rightarrow H_2 + CsBO_2$	1.2×10^{14}	1.00	0.00	
$HBO + CsOH \rightarrow H_2 + CsBO_2$	4.2×10^{14}	1.00	0.00	
$B_2O + CsOH \rightarrow BH + CsBO_2$	2.4×10^{14}	1.00	0.00	
$B_2O_2 + CsOH \rightarrow BOH + CsBO_2$	1.4×10^{14}	1.00	0.00	
$B_2O_2 + CsOH \rightarrow HBO + CsBO_2$	1.4×10^{14}	1.00	0.00	
$IO + MoO_2 \rightarrow I + MoO_3$	2.1×10^{14}	1.00	0.00	
$HOI + MoO_2 \rightarrow HI + MoO_3$	3.4×10^{14}	1.00	0.00	
$MoO + MoO_2 \rightarrow Mo + MoO_3$	2.0×10^{14}	1.00	0.00	
$MoO_2 + MoO_2 \rightarrow MoO + MoO_3$	6.4×10^{13}	1.00	6.61×10^{4}	
$BO + MoO_2 \rightarrow B + MoO_3$	2.6×10^{14}	1.00	3.20×10^{5}	
$BO_2 + MoO \rightarrow B + MoO_3$	4.9×10^{13}	1.00	2.69×10^{5}	
$BO_2 + MoO_2 \rightarrow BO + MoO_3$	1.7×10^{14}	1.00	1.46×10^{4}	
$B_2O3 + Mo \rightarrow B_2 + MoO_3$	1.2×10^{14}	1.00	1.04×10^{6}	
$B_2O3 + MoO \rightarrow B_2O + MoO_3$	5.3×10^{12}	-0.15	4.76×10^{5}	
$B_2O3 + MoO_2 \rightarrow B_2O_2 + MoO_3$	3.0×10^{11}	-0.85	3.08×10^{5}	
$HBO_2 + MoO \rightarrow BH + MoO_3$	1.4×10^{14}	1.00	4.31×10^{5}	
$HBO_2 + MoO_2 \rightarrow BOH + MoO_3$	1.0×10^{14}	1.00	2.54×10^{5}	
$HBO + MoO_2 \rightarrow BH + MoO_3$	3.0×10^{14}	1.00	4.42×10^{5}	
$B_2O + MoO_2 \rightarrow B_2 + MoO_3$	4.1×10^{14}	1.00	5.71×10^{5}	
$B_2O_2 + MoO \rightarrow B_2 + MoO_3$	5.6×10^{14}	1.00	8.90×10^{5}	
$B_2O_2 + MoO_2 \rightarrow B_2O + MoO_3$	4.0×10^{11}	-0.28	4.01×10^{5}	
$O_2 + MoO + M \rightarrow MoO_3 + M$	4.7×10^{16}	2.00	0.00	
$MoO_3 + (MoO_3)_2 + M \rightarrow (MoO_3)_3 + M$	1.5×10^{16}	2.00	0.00	
$MoO_3 + (MoO_3)_3 + M \rightarrow (MoO_3)_4 + M$	6.4×10^{15}	2.00	0.00	

Chemical reactions	A [a] (cm^3/mol-s)	n	E (J/mol)	Ref.
$MoO_3 + (MoO_3)_4 + M \rightarrow (MoO_3)_5 + M$	1.1×10^{16}	2.00	0.00	
$(MoO_3)_2 + (MoO_3)_2 \rightarrow MoO_3 + (MoO_3)_3$	1.2×10^{14}	1.00	3.28×10^{4}	
$MoO_4 + H_2O \rightarrow H_2MoO_4 + O$	2.7×10^{19}	-3.28	4.18×10^{5}	
$MoO_4 + H_2 + M \rightarrow H_2MoO_4 + M$	4.4×10^{13}	2.00	0.00	
$MoO_4 + H_2BO_2 \rightarrow H_2MoO_4 + BO_2$	1.4×10^{14}	1.00	0.00	
$MoO_4 + H_2O_2 \rightarrow H_2MoO_4 + O_2$	5.3×10^{14}	1.00	0.00	
$MoO_3 + H_2O + M \rightarrow H_2MoO_4 + M$	4.4×10^{13}	2.00	0.00	
$MoO_3 + H_2BO_2 \rightarrow H_2MoO_4 + BO$	2.1×10^{14}	1.00	0.00	
$MoO_3 + H_3BO_3 \rightarrow H2MoO_4 + HBO_2$	1.3×10^{14}	1.00	0.00	
$MoO_3 + H_2O_2 \rightarrow H_2MoO_4 + O$	5.3×10^{14}	1.00	0.00	
$MoO_2 + I_2 + M \rightarrow I_2MoO_2 + M$	1.2×10^{16}	2.00	0.00	
$MoO_2 + MoI_2 \rightarrow I_2MoO_2 + Mo$	3.0×10^{13}	1.00	0.00	
$MoI_2 + O_2 + M \rightarrow I_2MoO_2 + M$	1.2×10^{16}	2.00	0.00	
$MoI_2 + HO_2 \rightarrow I_2MoO_2 + H$	1.4×10^{14}	1.00	0.00	
$MoI_2 + BO_2 \rightarrow I_2MoO_2 + B$	1.1×10^{14}	1.00	2.68×10^{5}	
$MoI_2 + HBO_2 \rightarrow I_2MoO_2 + BH$	1.4×10^{14}	1.00	4.30×10^{5}	
$MoI_2 + H_2BO_2 \rightarrow I_2MoO_2 + BH_2$	1.4×10^{14}	1.00	1.68×10^{5}	
$MoI_2 + MoO_3 \rightarrow I_2MoO_2 + MoO$	1.2×10^{12}	1.00	0.00	
$MoI_2 + MoO_4 \rightarrow I_2MoO_2 + MoO_2$	1.2×10^{14}	1.00	0.00	
$MoI_2 + H_2O_2 \rightarrow I_2MoO_2 + H_2$	1.4×10^{14}	1.00	0.00	

[a] For three-body reactions, A has units of cm^6/mol^2-s.

[b] The effect of third body was eliminated in the rate expressions in ref. [84].

b. Thermodynamic data constants (C_p: heat capacity, $H°$: enthalpy, $S°$: entropy) for Cs-I-B-Mo-O-H system

$$\frac{C_p}{R} = a_1 + a_2T + a_3T^2 + a_4T^3 + a_5T^4,\ \frac{H^\circ}{RT} = a_1 + \frac{a_2}{2}T + \frac{a_3}{3}T^2 + \frac{a_4}{4}T^3 + \frac{a_5}{5}T^4 + \frac{a_6}{T}$$

$$\frac{S^\circ}{R} = a_1 lnT + a_2T + \frac{a_3}{2}T^2 + \frac{a_4}{3}T^3 + \frac{a_5}{4}T^4 + a_7$$

Species	a_1*	a_2*	a_3*	a_4*	a_5*	a_6*	a_7*
Ar	2.5000E+00	0.0000E+00	0.0000E+00	0.0000E+00	0.0000E+00	-7.4537E+02	4.3661E+00
	2.5000E+00	0.0000E+00	0.0000E+00	0.0000E+00	0.0000E+00	-7.4537E+02	4.3661E+00
B	2.4691E+00	6.9906E-05	-5.6544E-08	1.8378E-11	-2.0507E-15	6.7221E+04	4.3665E+00
	2.4796E+00	1.0527E-04	-1.5527E-07	9.0414E-11	-1.8750E-14	6.7211E+04	4.2878E+00
$CsBO_2$	6.0385E+00	5.8464E-03	-3.5778E-06	1.0071E-09	-1.0711E-13	-8.4659E+04	1.8741E+00
	4.6925E+00	1.0884E-02	-1.0063E-05	4.5331E-09	-8.0205E-13	-8.4418E+04	8.3700E+00
HB	2.6607E+00	2.7351E-03	-2.0512E-06	7.9263E-10	-1.0053E-13	5.2732E+04	4.7511E+00
	3.7146E+00	-1.6469E-03	3.9022E-06	-2.5518E-09	5.7327E-13	5.2592E+04	-1.7178E-01
BOH	4.8581E+00	7.8200E-04	3.7287E-07	-2.5378E-10	3.7394E-14	-2.5260E+03	-2.2230E+00
	2.8843E+00	5.6753E-03	-4.1502E-06	1.5920E-09	-2.4281E-13	-1.8922E+03	8.2385E+00
HBO	2.1997E+00	6.9689E-03	-3.9941E-06	1.0854E-09	-1.1344E-13	-2.6149E+04	1.0152E+01
	2.5777E+00	6.9109E-03	-4.8863E-06	1.9042E-09	-3.2031E-13	-2.6369E+04	7.8186E+00
HBO_2	4.6184E+00	5.4816E-03	-2.4696E-06	5.3854E-10	-4.6206E-14	-6.9101E+04	8.0465E-01
	2.4845E+00	1.2240E-02	-1.0295E-05	4.4912E-09	-7.8407E-13	-6.8581E+04	1.1564E+01
H_2B	2.5344E+00	5.5604E-03	-2.7507E-06	6.2588E-10	-5.4479E-14	3.7237E+04	7.2158E+00
	3.9721E+00	-7.5462E-04	6.0455E-06	-4.3863E-09	9.6469E-13	3.7085E+04	6.2743E-01
H_2BO	3.4456E+00	7.0806E-03	-3.4315E-06	8.1192E-10	-7.5911E-14	-8.3932E+03	6.6071E+00
	2.6144E+00	1.0941E-02	-8.9365E-06	3.9893E-09	-7.2726E-13	-8.3288E+03	1.0338E+01
H_2BO_2	3.4267E+00	1.1640E-02	-6.3209E-06	1.6457E-09	-1.6597E-13	-5.3571E+04	9.0063E+00
	1.4026E+00	2.3466E-02	-2.4576E-05	1.2616E-08	-2.4706E-12	-5.3687E+04	1.7181E+01
H_3B	4.0563E+00	3.7128E-03	-2.9271E-07	-2.8853E-10	5.8193E-14	8.7447E+03	-2.5261E+00
	3.6354E+00	-2.8653E-04	8.8282E-06	-6.6185E-09	1.4926E-12	9.4472E+03	1.5954E+00
H_3BO	3.4993E+00	9.4721E-03	-4.0797E-06	8.3063E-10	-6.4905E-14	-3.6475E+04	4.7105E+00
	1.4327E+00	1.4933E-02	-9.4907E-06	3.2133E-09	-4.5831E-13	-3.5849E+04	1.5538E+01
H_3BO_2	2.3611E+00	1.7007E-02	-9.3749E-06	2.4671E-09	-2.5117E-13	-7.8517E+04	1.3393E+01
	3.2055E-01	2.9371E-02	-2.8661E-05	1.4116E-08	-2.7054E-12	-7.8684E+04	2.1468E+01
H_3BO_3	2.2141E+00	2.1799E-02	-1.2484E-05	3.3884E-09	-3.5310E-13	-1.2162E+05	1.4887E+01
	-1.7387E-01	3.9497E-02	-4.1513E-05	2.1326E-08	-4.1820E-12	-1.2217E+05	2.3126E+01

Species	a_1^*	a_2^*	a_3^*	a_4^*	a_5^*	a_6^*	a_7^*
BI	2.7897E+00	3.2994E-03	-2.2885E-06	6.9551E-10	-7.4551E-14	3.7173E+04	1.1657E+01
	3.2576E+00	3.8925E-03	-4.7225E-06	2.5955E-09	-5.2758E-13	3.6825E+04	8.5192E+00
BI_2	5.3393E+00	2.9544E-03	-2.0734E-06	6.5968E-10	-7.6333E-14	2.5770E+04	6.3706E+00
	4.4598E+00	7.7216E-03	-9.2624E-06	4.9312E-09	-9.6764E-13	2.5761E+04	1.0062E+01
BI_3	6.3870E+00	6.5077E-03	-4.4284E-06	1.3261E-09	-1.4677E-13	7.6413E+02	4.6246E+00
	6.1722E+00	1.1509E-02	-1.3858E-05	7.4850E-09	-1.5013E-12	3.3040E+02	4.0875E+00
BO	3.7135E+00	4.3770E-04	6.3111E-08	-8.2971E-11	1.4274E-14	-1.0755E+02	2.8618E+00
	3.5163E+00	-7.3295E-04	2.9303E-06	-2.1113E-09	4.7799E-13	1.4247E+02	4.5293E+00
BO_2	5.7036E+00	2.2513E-03	-1.1806E-06	3.0055E-10	-2.9933E-14	-3.9204E+04	-5.9843E+00
	2.9016E+00	1.0257E-02	-9.7196E-06	4.3328E-09	-7.4149E-13	-3.8423E+04	8.4697E+00
B_2	4.3391E+00	7.2811E-04	-2.3178E-07	5.0051E-11	-4.8458E-15	9.9179E+04	-8.5766E-01
	1.5628E+00	1.0657E-02	-1.2687E-05	6.7083E-09	-1.3017E-12	9.9728E+04	1.2715E+01
$H_4B_2O_4$	4.0962E+00	3.0742E-02	-1.7703E-05	4.8156E-09	-5.0214E-13	-1.5498E+05	1.1600E+01
	1.8660E-01	5.7199E-02	-6.0191E-05	3.0824E-08	-6.0243E-12	-1.5561E+05	2.6035E+01
H_6B_2	3.6404E+00	2.1295E-02	-1.0709E-05	2.5755E-09	-2.4141E-13	1.8119E+03	-4.2252E-02
	-6.9887E-01	3.0248E-02	-1.7044E-05	4.2270E-09	-3.2271E-13	3.4083E+03	2.3633E+01
B_2O	5.9507E+00	2.1476E-03	-1.2449E-06	3.3572E-10	-3.4520E-14	1.8622E+04	-7.6682E+00
	3.7111E+00	8.8809E-03	-8.7394E-06	4.0049E-09	-7.0243E-13	1.9208E+04	3.7591E+00
B_2O_2	4.8896E+00	8.0801E-03	-4.8239E-06	1.3257E-09	-1.3802E-13	-5.6667E+04	2.5857E-01
	5.1359E+00	9.0738E-03	-7.4683E-06	3.2346E-09	-5.7844E-13	-5.6927E+04	-1.6488E+00
B_2O_3	6.2843E+00	9.2348E-03	-5.4015E-06	1.4852E-09	-1.5681E-13	-1.0282E+05	-4.2530E+00
	3.8046E+00	1.7460E-02	-1.5240E-05	6.5747E-09	-1.1245E-12	-1.0226E+05	8.1107E+00
$B_3H_3O_3$	6.1387E+00	2.4846E-02	-1.3938E-05	3.6704E-09	-3.7074E-13	-1.4808E+05	-8.5702E+00
	-1.8086E+00	4.9683E-02	-4.2419E-05	1.7948E-08	-3.0203E-12	-1.4611E+05	3.1627E+01
$B_3H_3O_6$	8.0704E+00	3.5337E-02	-2.0602E-05	5.6117E-09	-5.8351E-13	-2.7550E+05	-1.1602E+01
	8.5194E-02	7.2961E-02	-7.4555E-05	3.6849E-08	-6.9993E-12	-2.7494E+05	2.4036E+01
B_5H_9	9.6691E+00	3.4633E-02	-1.6918E-05	3.9223E-09	-3.5332E-13	2.5876E+03	-3.5757E+01
	-6.7014E+00	7.4482E-02	-5.2962E-05	1.8250E-08	-2.4594E-12	7.9268E+03	5.1286E+01
$B_{10}H_{14}$	1.1163E+01	7.6424E-02	-4.2197E-05	1.0954E-08	-1.0942E-12	-2.2435E+03	-4.6064E+01
	-1.4972E+01	1.5852E-01	-1.3670E-04	5.8467E-08	-9.9317E-12	4.2013E+03	8.5963E+01
Cs	1.6296E+00	1.9834E-03	-1.6356E-06	5.5857E-10	-5.9812E-14	8.7543E+03	1.1540E+01
	2.5000E+00	-1.5809E-06	1.3486E-08	-2.5060E-11	1.2578E-14	8.4554E+03	6.8628E+00
CsH	3.4627E+00	1.6288E-03	-8.0662E-07	2.1384E-10	-2.4072E-14	1.2888E+04	5.7369E+00
	2.7738E+00	4.7680E-03	-5.2480E-06	2.7665E-09	-5.4597E-13	1.2948E+04	8.8513E+00

Species	a_1^*	a_2^*	a_3^*	a_4^*	a_5^*	a_6^*	a_7^*
CsOH	2.7069E+00	6.9277E-03	-4.3549E-06	1.2648E-09	-1.3804E-13	-3.1301E+04	1.4465E+01
	5.0060E+00	4.8781E-03	-6.3867E-06	3.9818E-09	-8.9318E-13	-3.2450E+04	9.1093E-01
CsI	4.2892E+00	5.1084E-04	-3.0010E-07	1.1063E-10	-1.2345E-14	-1.9581E+04	8.5903E+00
	4.3523E+00	7.2379E-04	-8.9432E-07	5.4417E-10	-1.1284E-13	-1.9643E+04	8.1173E+00
$CsMoO_4$	8.3734E+00	1.3190E-02	-8.7779E-06	2.5917E-09	-2.8408E-13	-8.3075E+04	-4.9960E+00
	6.5324E+00	2.6502E-02	-3.0492E-05	1.5977E-08	-3.1374E-12	-8.3468E+04	1.4809E+00
CsO	1.8617E+00	6.2948E-03	-4.7616E-06	1.5430E-09	-1.7920E-13	4.4283E+03	1.8910E+01
	2.2087E+00	1.3418E-02	-1.9934E-05	1.1864E-08	-2.4955E-12	3.4188E+03	1.4077E+01
Cs_2	1.2958E+01	-1.5114E-02	8.4204E-06	-1.8351E-09	1.3802E-13	8.5694E+03	-3.8240E+01
	3.7185E+00	4.5811E-03	-6.3321E-06	2.5250E-09	-2.2256E-13	1.1897E+04	1.1933E+01
$Cs_2O_2H_2$	8.1669E+00	1.0379E-02	-6.2320E-06	1.7770E-09	-1.9337E-13	-8.0519E+04	-1.8106E+00
	1.1235E+01	8.9221E-03	-1.1500E-05	7.1072E-09	-1.5799E-12	-8.2196E+04	-2.0378E+01
Cs_2I_2	9.7773E+00	4.1697E-04	-2.8948E-07	8.7733E-11	-9.7871E-15	-5.7508E+04	-3.9157E+00
	9.8265E+00	5.8959E-04	-7.6579E-07	4.3441E-10	-9.0062E-14	-5.7557E+04	-4.2867E+00
Cs_2MoO_4	9.8529E+00	1.6356E-02	-1.1128E-05	3.3427E-09	-3.7169E-13	-1.4787E+05	-6.9221E+00
	9.0457E+00	2.8972E-02	-3.4209E-05	1.8252E-08	-3.6316E-12	-1.4880E+05	-6.6248E+00
Cs_2O	5.2641E+00	3.2310E-03	-2.2397E-06	6.7883E-10	-7.5758E-14	-1.8644E+04	8.5545E+00
	5.6524E+00	4.5335E-03	-5.8801E-06	3.3359E-09	-6.9177E-13	-1.9023E+04	5.6471E+00
Cs_2O_2	7.0261E+00	5.3443E-03	-3.6338E-06	1.0879E-09	-1.2041E-13	-3.1739E+04	3.5534E-02
	6.8540E+00	9.3772E-03	-1.1241E-05	6.0573E-09	-1.2134E-12	-3.2090E+04	-4.0470E-01
H	2.5000E+00	0.0000E+00	0.0000E+00	0.0000E+00	0.0000E+00	2.5474E+04	-4.5972E-01
	2.5000E+00	0.0000E+00	0.0000E+00	0.0000E+00	0.0000E+00	2.5474E+04	-4.5972E-01
HI	4.1744E+00	-8.4835E-04	1.1095E-06	-4.1530E-10	5.2094E-14	1.7538E+03	8.3678E-01
	3.7223E+00	-1.7185E-03	4.0555E-06	-2.6472E-09	5.7784E-13	2.1229E+03	3.9797E+00
HIO	3.0074E+00	5.0062E-03	-2.9120E-06	8.2423E-10	-9.0370E-14	-1.0441E+04	1.2511E+01
	3.2547E+00	6.5016E-03	-6.5622E-06	3.4042E-09	-6.7998E-13	-1.0757E+04	1.0409E+01
HMoO	4.0688E+00	3.8963E-03	-1.9923E-06	4.7553E-10	-3.7359E-14	3.9786E+04	6.9913E+00
	3.9275E+00	7.5995E-03	-9.0218E-06	5.0781E-09	-1.0508E-12	3.9454E+04	6.4831E+00
$HMoO_2$	5.3167E+00	5.6636E-03	-3.0984E-06	8.2217E-10	-8.4158E-14	-1.7354E+04	3.2951E+00
	3.4461E+00	1.3990E-02	-1.4763E-05	7.4897E-09	-1.4427E-12	-1.7168E+04	1.1827E+01
HO	2.3572E+00	2.0390E-03	-9.7535E-07	2.6405E-10	-2.9289E-14	4.1423E+03	8.5037E+00
	3.8865E+00	-1.5156E-03	2.0558E-06	-8.5043E-10	1.1768E-13	3.6247E+03	3.0918E-01
HO_2	4.7139E+00	1.0426E-03	1.4390E-07	-1.2354E-10	1.6248E-14	-5.3874E+02	-1.5680E-01
	3.0652E+00	4.3828E-03	-2.1400E-06	4.2208E-10	3.5550E-15	7.4696E+01	8.8618E+00

Species	a_1^*	a_2^*	a_3^*	a_4^*	a_5^*	a_6^*	a_7^*
H_2	2.5737E+00	1.2804E-03	-3.3988E-07	4.9514E-11	-2.8840E-15	-6.1623E+02	1.0792E+00
	3.3028E+00	9.3292E-04	-1.5892E-06	1.3145E-09	-3.3199E-13	-1.0146E+03	-3.3326E+00
H_2MoO_2	6.0085E+00	7.4876E-03	-3.7007E-06	9.0537E-10	-8.5120E-14	-9.1143E+03	-2.2734E-01
	4.2522E+00	1.6608E-02	-1.7258E-05	8.9030E-09	-1.7467E-12	-9.0866E+03	7.2939E+00
H_2MoO_3	7.0359E+00	1.0768E-02	-5.7981E-06	1.5323E-09	-1.5819E-13	-5.9951E+04	-3.1911E+00
	4.6505E+00	2.3670E-02	-2.5242E-05	1.3081E-08	-2.5675E-12	-5.9971E+04	6.8316E+00
H_2MoO_4	8.4945E+00	1.3447E-02	-7.6326E-06	2.0690E-09	-2.1670E-13	-1.0506E+05	-1.1182E+01
	5.2658E+00	3.0247E-02	-3.2624E-05	1.6816E-08	-3.2813E-12	-1.0501E+05	2.6318E+00
H_2O	2.3046E+00	3.7542E-03	-1.3668E-06	2.8777E-10	-2.6831E-14	-2.9742E+04	8.9098E+00
	3.9931E+00	-5.2845E-04	2.6960E-06	-1.4202E-09	2.4155E-13	-3.0273E+04	-2.9219E-03
H_2O_2	3.1980E+00	1.0073E-02	-9.6539E-06	4.9375E-09	-9.9413E-13	-1.7729E+04	7.0820E+00
	2.8691E+00	7.6232E-03	4.8732E-06	-1.7734E-08	1.0258E-11	-1.7577E+04	9.3094E+00
I	2.3290E+00	3.8820E-04	-3.4840E-07	1.4692E-10	-2.0426E-14	1.2156E+04	8.4100E+00
	2.4901E+00	6.2403E-05	-1.2636E-07	9.4355E-11	-1.9352E-14	1.2096E+04	7.5286E+00
MoI	3.0548E+00	2.8765E-03	-1.9982E-06	5.9455E-10	-5.6399E-14	5.9343E+04	1.5665E+01
	4.1236E+00	1.5052E-03	-2.1061E-06	1.2999E-09	-2.8352E-13	5.8856E+04	9.5206E+00
IO	4.8535E+00	1.0230E-04	5.6233E-08	-5.9711E-11	8.7425E-15	1.3409E+04	5.1623E-01
	3.1746E+00	3.0327E-03	-1.3274E-06	-1.3215E-10	1.3538E-13	1.4087E+04	9.8766E+00
IOO	6.1103E+00	9.2017E-04	-3.8943E-07	7.4008E-11	-5.0485E-15	1.2004E+04	2.4798E-01
	5.1775E+00	2.7049E-03	-1.4714E-06	2.4258E-10	1.8908E-14	1.2363E+04	5.3898E+00
OIO	4.3192E+00	4.6837E-03	-3.1366E-06	9.3014E-10	-1.0226E-13	2.2201E+04	8.2740E+00
	3.6049E+00	9.5957E-03	-1.1056E-05	5.7863E-09	-1.1344E-12	2.2077E+04	1.0882E+01
IO_3	4.6277E+00	9.4898E-03	-6.3957E-06	1.9043E-09	-2.0994E-13	2.7755E+04	7.0196E+00
	3.4483E+00	1.8996E-02	-2.2263E-05	1.1784E-08	-2.3277E-12	2.7394E+04	1.0802E+01
I_2	6.0001E+00	-3.1182E-03	2.3234E-06	-6.3955E-10	5.8144E-14	5.6102E+03	-2.4983E+00
	4.2485E+00	9.0418E-04	-1.0503E-06	5.7154E-10	-9.5649E-14	6.2087E+03	6.9060E+00
MoI_2	6.5047E+00	1.8294E-03	-1.3117E-06	4.3722E-10	-4.8799E-14	2.9411E+04	2.6634E+00
	6.7544E+00	2.6693E-03	-3.6574E-06	2.1491E-09	-4.4565E-13	2.9167E+04	7.9263E-01
I_2MoO_2	9.1420E+00	6.3620E-03	-4.1199E-06	1.1953E-09	-1.2945E-13	-3.8920E+04	-8.4215E+00
	7.5326E+00	1.4244E-02	-1.5591E-05	7.8893E-09	-1.5110E-12	-3.8841E+04	-1.3507E+00
IIO	5.4603E+00	2.7367E-03	-1.8498E-06	5.5181E-10	-6.0926E-14	1.1220E+04	8.1327E+00
	5.2290E+00	5.1497E-03	-6.0592E-06	3.2210E-09	-6.3886E-13	1.1087E+04	8.6683E+00
IOI	4.5198E+00	4.5994E-03	-3.1832E-06	9.6408E-10	-1.0758E-13	1.3138E+04	1.0610E+01
	4.8716E+00	6.7626E-03	-8.4477E-06	4.6822E-09	-9.5700E-13	1.2684E+04	7.6071E+00

Species	a_1*	a_2*	a_3*	a_4*	a_5*	a_6*	a_7*
MoI_3	8.9049E+00	1.9903E-03	-1.3678E-06	4.3346E-10	-4.8375E-14	1.9066E+04	-2.9985E+00
	9.1521E+00	2.8246E-03	-3.6955E-06	2.1317E-09	-4.4204E-13	1.8823E+04	-4.8512E+00
MoI_4	1.2136E+01	1.5111E-03	-8.1628E-07	2.3477E-10	-2.6210E-14	1.1436E+04	-1.1048E+01
	1.2271E+01	1.9569E-03	-2.0686E-06	1.1498E-09	-2.3845E-13	1.1304E+04	-1.2058E+01
MoI_5	7.6605E+00	1.7819E-02	-1.3229E-05	4.1754E-09	-4.7824E-13	1.6738E+04	1.2181E+01
	1.0667E+01	2.6216E-02	-3.8040E-05	2.2498E-08	-4.7478E-12	1.3989E+04	-9.6964E+00
MoI_6	1.6242E+01	5.1574E-03	-3.5803E-06	1.0856E-09	-1.2116E-13	2.7804E+04	-2.9643E+01
	1.6862E+01	7.2403E-03	-9.4009E-06	5.3337E-09	-1.1060E-12	2.7197E+04	-3.4291E+01
Mo	1.6962E+00	1.7947E-03	-1.4434E-06	4.7322E-10	-4.5128E-14	7.8629E+04	1.1962E+01
	2.4949E+00	2.7795E-05	-3.9391E-08	1.0545E-11	5.1012E-15	7.8348E+04	7.6490E+00
MoO	4.6558E+00	-2.7838E-04	1.4152E-07	-1.2190E-11	1.2787E-15	4.1462E+04	2.7485E+00
	4.1379E+00	3.7532E-04	2.1516E-07	-3.6818E-10	1.1449E-13	4.1699E+04	5.7298E+00
MoO_2	4.1119E+00	4.6739E-03	-3.0010E-06	8.9202E-10	-9.7313E-14	-3.1852E+03	8.3528E+00
	2.4702E+00	1.2142E-02	-1.3558E-05	6.9575E-09	-1.3371E-12	-3.0403E+03	1.5780E+01
MoO_3	5.0622E+00	8.5102E-03	-5.6757E-06	1.6805E-09	-1.8414E-13	-4.5409E+04	2.5174E+00
	3.1356E+00	1.9067E-02	-2.1652E-05	1.1190E-08	-2.1704E-12	-4.5441E+04	1.0561E+01
MoO_4	6.3037E+00	1.1491E-02	-7.6123E-06	2.2409E-09	-2.4510E-13	-2.4904E+04	-8.3341E-01
	4.4890E+00	2.3527E-02	-2.6846E-05	1.3988E-08	-2.7361E-12	-2.5170E+04	5.9579E+00
Mo_2	9.3618E+00	-9.0345E-03	5.1063E-06	-7.1202E-10	-9.2849E-15	1.0545E+05	-2.3320E+01
	3.5393E+00	3.0305E-03	-3.4973E-06	1.5734E-09	-1.3378E-13	1.0758E+05	8.4285E+00
Mo_2O_6	1.0278E+01	2.0341E-02	-1.3583E-05	4.0227E-09	-4.4190E-13	-1.4138E+05	-1.6258E+01
	6.5026E+00	4.3596E-02	-5.0027E-05	2.6082E-08	-5.0953E-12	-1.4173E+05	-1.4609E+00
Mo_3O_9	1.8044E+01	2.7342E-02	-1.8136E-05	5.3488E-09	-5.8594E-13	-2.3440E+05	-4.7746E+01
	1.1682E+01	6.1621E-02	-6.9728E-05	3.5974E-08	-6.9726E-12	-2.3443E+05	-2.0967E+01
Mo_4O_{12}	2.4152E+01	3.7649E-02	-2.5048E-05	7.4011E-09	-8.1179E-13	-3.2323E+05	-7.2513E+01
	1.6191E+01	8.2971E-02	-9.4463E-05	4.8959E-08	-9.5228E-12	-3.2355E+05	-3.9910E+01
Mo_5O_{15}	3.0531E+01	4.7357E-02	-3.1515E-05	9.3130E-09	-1.0216E-12	-4.0980E+05	-9.8941E+01
	2.0607E+01	1.0416E-01	-1.1866E-04	6.1527E-08	-1.1971E-11	-4.1024E+05	-5.8414E+01
O	2.9946E+00	-9.0737E-04	6.1892E-07	-1.8525E-10	2.0706E-14	2.9048E+04	2.4191E+00
	2.8864E+00	-1.2513E-03	1.5953E-06	-9.0030E-10	1.8673E-13	2.9151E+04	3.2223E+00
O_2	4.9746E+00	-1.8212E-03	1.5866E-06	-5.0780E-10	5.8365E-14	-1.7599E+03	-3.9068E+00
	3.2390E+00	7.3184E-04	1.1088E-06	-1.2178E-09	3.3042E-13	-1.0058E+03	5.9483E+00
O_3	-4.3254E+00	2.5838E-02	-2.2273E-05	8.3786E-09	-1.0700E-12	1.8258E+04	4.8457E+01
	2.2083E+00	1.1231E-02	-1.0484E-05	4.3907E-09	-6.1396E-13	1.5981E+04	1.3230E+01

* upper row: temperature range from 1500 to 3000 K, lower row: temperature range from 298.15 to 1500 K

c. Dataset of chemical reaction rate constants k for Ru-N-O-H system

$$k = AT^n \exp\left(-\frac{E}{\mathrm{R}T}\right)$$

Chemical reactions	A [a] (cm^3/mol-s)	n	E (J/mol)	Ref.
$NO_2 + OH + M \rightarrow HNO_3 + M$	1.1×10^{28}	-4.01	0.00	[90]
$NO + O + M \rightarrow NO_2 + M$	3.3×10^{20}	-1.60	0.00	[91]
$NO_3 + NO_3 \rightarrow NO_2 + NO_2 + O_2$	5.1×10^{11}	0.00	2.04×10^{4}	[92]
$NO_3 + NO_2 \rightarrow NO + O_2 + NO_2$	1.5×10^{10}	0.00	1.02×10^{4}	[92]
$NO + M \rightarrow N + O + M$	1.4×10^{15}	0.00	6.21×10^{5}	[93]
$HNO + H \rightarrow NO + H_2$	4.5×10^{11}	0.72	2.74×10^{3}	[93]
$N + O_2 \rightarrow NO + O$	5.8×10^{9}	1.01	2.59×10^{4}	[91]
$HNO + M \rightarrow NO + H + M$	2.6×10^{16}	0.00	2.04×10^{5}	[93]
$N + OH \rightarrow NO + H$	1.1×10^{14}	-0.20	0.00	[91]
$N_2O + O \rightarrow NO + NO$	9.0×10^{13}	0.00	1.16×10^{5}	[91]
$HONO + H \rightarrow NO_2 + H_2$	2.0×10^{8}	1.55	2.77×10^{4}	[93]
$NO_2 + O \rightarrow NO + O_2$	3.9×10^{12}	0.00	-9.98×10^{2}	[93]
$NO_2 + O + M \rightarrow NO_3 + M$	1.5×10^{28}	-4.08	1.03×10^{4}	[94]
$NO_2 + H \rightarrow NO + OH$	8.8×10^{13}	0.00	0.00	[95]
$NO + HO_2 \rightarrow NO_2 + OH$	2.0×10^{12}	0.00	-2.08×10^{3}	[91]
$NO_2 + NO_2 \rightarrow NO_3 + NO$	9.6×10^{9}	-0.73	8.75×10^{4}	[94]
$NO_2 + NO_2 \rightarrow NO + NO + O_2$	1.6×10^{12}	0.00	1.09×10^{5}	[94]
$HNO + O \rightarrow NO + OH$	4.5×10^{11}	0.72	2.74×10^{3}	[93]
$HNO + OH \rightarrow NO + H_2O$	1.3×10^{7}	1.88	-3.99×10^{3}	[93]
$HNO + HNO \rightarrow N_2O + H_2O$	8.5×10^{8}	0.00	1.29×10^{4}	[93]
$N_2O + M \rightarrow N_2 + O + M$	5.7×10^{14}	0.00	2.35×10^{5}	[93]
$N_2O + O \rightarrow N_2 + O_2$	3.7×10^{12}	0.00	6.67×10^{4}	[91]
$N_2O + H \rightarrow N_2 + OH$	2.2×10^{14}	0.00	7.01×10^{4}	[93]
$NO + N \rightarrow N_2 + O$	9.4×10^{12}	0.14	0.00	[96]
$N_2O + OH \rightarrow N_2 + HO_2$	1.3×10^{-2}	4.72	1.53×10^{5}	[93]
$HNO + NO \rightarrow N_2O + OH$	8.5×10^{12}	0.00	1.24×10^{5}	[93]
$HNO + O_2 \rightarrow NO + HO_2$	2.0×10^{13}	0.00	6.65×10^{4}	[93]
$HONO + M \rightarrow NO + OH + M$	2.0×10^{31}	-4.56	2.14×10^{5}	[93]

Chemical reactions	A [a] (cm^3/mol-s)	n	E (J/mol)	Ref.
$HONO + H \rightarrow NO + H_2O$	8.1×10^{6}	1.89	1.61×10^{4}	[93]
$HONO + H \rightarrow HNO + OH$	5.6×10^{10}	0.86	2.08×10^{4}	[93]
$HONO + O \rightarrow OH + NO_2$	1.7×10^{8}	1.50	1.27×10^{4}	[93]
$HONO + OH \rightarrow NO_2 + H_2O$	1.2×10^{6}	2.00	-2.49×10^{3}	[93]
$NO_3 + O \rightarrow NO_2 + O_2$	1.0×10^{13}	0.00	0.00	[97]
$HNO_3 + OH \rightarrow NO_3 + H_2O$	8.7×10^{0}	3.50	-6.98×10^{3}	[98]
$NO_3 + OH \rightarrow NO_2 + HO_2$	1.2×10^{13}	0.00	0.00	[97]
$NO_3 + HO_2 \rightarrow NO_2 + O_2 + OH$	2.4×10^{12}	0.00	0.00	[97]
$OH + OH \rightarrow H_2O + O$	1.5×10^{9}	1.14	4.20×10^{2}	[79]
$OH + H_2 \rightarrow H_2O + H$	1.8×10^{9}	1.21	1.97×10^{4}	[79]
$O + H_2 \rightarrow OH + H$	5.1×10^{4}	2.67	2.63×10^{4}	[79]
$O + OH \rightarrow O_2 + H$	2.8×10^{11}	0.40	-3.09×10^{3}	[79]
$H_2O + M \rightarrow H + OH + M$	1.3×10^{15}	0.00	4.40×10^{5}	[86]
$OH + M \rightarrow O + H + M$	2.4×10^{15}	0.00	4.16×10^{5}	[79]
$HO_2 + H \rightarrow H_2 + O_2$	6.7×10^{7}	1.77	-2.38×10^{3}	[79]
$HO_2 + H \rightarrow H_2O + O$	9.1×10^{8}	1.47	5.81×10^{4}	[79]
$HO_2 + H \rightarrow OH + OH$	2.2×10^{11}	0.88	-2.70×10^{2}	[79]
$HO_2 + OH \rightarrow H_2O + O_2$	2.9×10^{13}	0.00	-2.08×10^{3}	[79]
$H_2 + M \rightarrow H + H + M$	2.2×10^{14}	0.00	4.02×10^{5}	[87]
$O_2 + M \rightarrow O + O + M$	1.8×10^{18}	-1.00	4.94×10^{5}	[79]
$HO_2 + O \rightarrow OH + O_2$	3.2×10^{13}	0.00	0.00	[87]
$HO_2 + HO_2 \rightarrow H_2O_2 + O_2$	4.2×10^{14}	0.00	5.01×10^{4}	[87]
$H_2O_2 + M \rightarrow OH + OH + M$	1.8×10^{16}	0.00	1.80×10^{5}	[87]
$H_2O_2 + H \rightarrow H_2O + OH$	1.0×10^{13}	0.00	1.50×10^{4}	[87]
$H_2O_2 + H \rightarrow H_2 + HO_2$	1.7×10^{12}	0.00	1.57×10^{4}	[87]
$H_2O_2 + O \rightarrow HO_2 + OH$	6.6×10^{11}	0.00	1.66×10^{4}	[87]
$H_2O_2 + OH \rightarrow HO_2 + H_2O$	7.8×10^{12}	0.00	5.57×10^{3}	[87]
$OH + OH \rightarrow O_2 + H_2$	2.0×10^{13}	-1.30	2.29×10^{5}	[84]
$RuO_2 + OH \rightarrow RuO_3 + H$	2.4×10^{14}	1.00	1.10×10^{5}	
$RuO_2 + H_2O \rightarrow RuO_3 + H2$	2.1×10^{17}	-1.45	2.90×10^{5}	

Chemical reactions	A [a] (cm^3/mol-s)	n	E (J/mol)	Ref.
$RuO_2 + O_2 \rightarrow RuO_3 + O$	3.3×10^{7}	1.19	2.07×10^{5}	
$RuO_2 + O + M \rightarrow RuO_3 + M$	2.9×10^{16}	2.00	0.00	
$RuO_2 + NO \rightarrow RuO_3 + N$	3.5×10^{9}	0.83	4.95×10^{5}	
$RuO_2 + NO_2 \rightarrow RuO_3 + NO$	1.2×10^{14}	1.00	0.00	
$RuO_2 + N_2O \rightarrow RuO_3 + N_2$	3.2×10^{9}	0.97	2.51×10^{5}	
$RuO_2 + HNO_3 \rightarrow RuO_3 + HONO\text{-cis}$	1.3×10^{5}	1.55	3.07×10^{4}	
$RuO_2 + HNO_3 \rightarrow RuO_3 + HONO\text{-trans}$	1.5×10^{14}	1.00	1.54×10^{4}	
$RuO_2 + NO_3 \rightarrow RuO_3 + NO_2$	3.6×10^{14}	1.00	0.00	
$RuO_3 + OH \rightarrow RuO_4 + H$	4.9×10^{13}	-0.14	2.86×10^{5}	
$RuO_3 + H_2O \rightarrow RuO_4 + H_2$	3.8×10^{19}	-2.32	5.66×10^{5}	
$RuO_3 + O_2 \rightarrow RuO_4 + O$	9.1×10^{5}	1.32	2.88×10^{5}	
$RuO_3 + O + M \rightarrow RuO_4 + M$	7.4×10^{16}	2.00	0.00	
$RuO_3 + NO \rightarrow RuO_4 + N$	1.5×10^{13}	-1.05	5.30×10^{5}	
$RuO_3 + NO_2 \rightarrow RuO_4 + NO$	2.6×10^{3}	2.72	2.37×10^{4}	
$RuO_3 + N_2O \rightarrow RuO_4 + N_2$	1.6×10^{6}	1.52	4.57×10^{1}	
$RuO_3 + HNO_3 \rightarrow RuO_4 + HONO\text{-cis}$	1.2×10^{7}	0.66	5.22×10^{4}	
$RuO_3 + HNO_3 \rightarrow RuO_4 + HONO\text{-trans}$	1.4×10^{7}	0.69	6.41×10^{4}	
$RuO_3 + NO_3 \rightarrow RuO_4 + NO_2$	1.9×10^{13}	-1.16	1.72×10^{5}	
$RuO_2 + HNO \rightarrow RuO_3 + NH$	3.9×10^{15}	1.00	1.93×10^{5}	
$RuO_3 + HNO \rightarrow RuO_4 + NH$	1.6×10^{8}	0.64	5.50×10^{5}	
$RuO_2 + HONO\text{-cis} \rightarrow RuO_3 + HNO$	1.8×10^{4}	2.27	2.94×10^{5}	
$RuO_2 + HONO\text{-trans} \rightarrow RuO_3 + H + NO$	1.1×10^{4}	2.22	3.71×10^{5}	
$RuO_3 + HONO\text{-cis} \rightarrow RuO_4 + HNO$	8.9×10^{11}	-1.13	3.40×10^{5}	
$RuO_3 + HONO\text{-trans} \rightarrow RuO_4 + H + NO$	4.1×10^{7}	1.13	3.88×10^{5}	
$NH_2 + H \rightarrow NH + H_2$	5.3×10^{13}	0.00	2.09×10^{4}	[91]
$NH + NO \rightarrow N_2O + H$	2.7×10^{15}	-0.78	3.33×10^{2}	[91]
$NH + NO \rightarrow N_2 + OH$	6.9×10^{14}	-0.78	3.33×10^{2}	[91]
$NH + O_2 \rightarrow NO + OH$	9.0×10^{10}	0.00	6.40×10^{3}	[91]
$NH + O_2 \rightarrow NO_2 + H$	2.3×10^{10}	0.00	1.04×10^{4}	[93]
$NH + O_2 \rightarrow HNO + O$	2.4×10^{13}	0.00	5.79×10^{4}	[91]

Chemical reactions	A [a] (cm^3/mol-s)	n	E (J/mol)	Ref.
$NH_2 + O_2 \rightarrow HNO + OH$	6.2×10^{7}	1.23	1.47×10^{5}	[93]
$NH_2 + O \rightarrow HNO + H$	4.6×10^{13}	0.00	0.00	[93]
$NH_2 + O \rightarrow NH + OH$	7.0×10^{12}	0.00	0.00	[93]
$NH_2 + OH \rightarrow NH + H_2O$	2.4×10^{6}	2.00	2.08×10^{2}	[93]
$NH_2 + NO \rightarrow N_2 + H_2O$	4.7×10^{12}	-0.25	-5.03×10^{3}	[93]
$NH + O \rightarrow N + OH$	1.7×10^{8}	1.50	1.41×10^{4}	[93]
$NH + N \rightarrow N_2 + H$	1.5×10^{13}	0.00	0.00	[93]
$NH_2 + N \rightarrow N_2 + 2H$	7.1×10^{13}	0.00	0.00	[93]
$NH + NH \rightarrow N2 + 2H$	5.1×10^{13}	0.00	0.00	[93]
$NH + OH \rightarrow HNO + H$	2.0×10^{13}	0.00	0.00	[93]
$NH + OH \rightarrow N + H_2O$	1.2×10^{6}	2.00	-2.04×10^{3}	[93]
$NH + H \rightarrow N + H_2$	3.0×10^{13}	0.00	0.00	[91]
$NH + O \rightarrow NO + H$	1.1×10^{14}	0.00	2.49×10^{3}	[91]
$NO_2 + NH_2 \rightarrow N_2O + H_2O$	1.7×10^{14}	-0.74	0.00	[91]
$NH_2 + O_2 \rightarrow NO + H_2O$	1.7×10^{14}	0.00	1.03×10^{5}	[91]
$NH_2 + HO_2 \rightarrow HNO + H_2O$	5.7×10^{15}	-1.12	2.96×10^{3}	[91]
$NH + NO \rightarrow N_2 + H + O$	4.5×10^{14}	0.00	8.76×10^{4}	[91]

d. Thermodynamic data constants (C_p: heat capacity, $H°$: enthalpy, $S°$: entropy) for Ru-N-O-H system

$$\frac{C_p}{R} = a_1 + a_2T + a_3T^2 + a_4T^3 + a_5T^4,\ \frac{H^\circ}{RT} = a_1 + \frac{a_2}{2}T + \frac{a_3}{3}T^2 + \frac{a_4}{4}T^3 + \frac{a_5}{5}T^4 + \frac{a_6}{T}$$

$$\frac{S^\circ}{R} = a_1 lnT + a_2T + \frac{a_3}{2}T^2 + \frac{a_4}{3}T^3 + \frac{a_5}{4}T^4 + a_7$$

Species	a_1*	a_2*	a_3*	a_4*	a_5*	a_6*	a_7*
Ar	2.5000E+00	0.0000E+00	0.0000E+00	0.0000E+00	0.0000E+00	-7.4537E+02	4.3661E+00
	2.5000E+00	0.0000E+00	0.0000E+00	0.0000E+00	0.0000E+00	-7.4537E+02	4.3661E+00
H	2.5000E+00	0.0000E+00	0.0000E+00	0.0000E+00	0.0000E+00	2.5474E+04	-4.5972E-01
	2.5000E+00	0.0000E+00	0.0000E+00	0.0000E+00	0.0000E+00	2.5474E+04	-4.5972E-01
OH	2.3572E+00	2.0390E-03	-9.7535E-07	2.6405E-10	-2.9289E-14	4.1423E+03	8.5037E+00
	3.8865E+00	-1.5156E-03	2.0558E-06	-8.5043E-10	1.1768E-13	3.6247E+03	3.0918E-01
HO_2	4.7139E+00	1.0426E-03	1.4390E-07	-1.2354E-10	1.6248E-14	-5.3874E+02	-1.5680E-01
	3.0652E+00	4.3828E-03	-2.1400E-06	4.2208E-10	3.5550E-15	7.4696E+01	8.8618E+00
H_2	2.5737E+00	1.2804E-03	-3.3988E-07	4.9514E-11	-2.8840E-15	-6.1623E+02	1.0792E+00
	3.3028E+00	9.3292E-04	-1.5892E-06	1.3145E-09	-3.3199E-13	-1.0146E+03	-3.3326E+00
H_2O	2.3046E+00	3.7542E-03	-1.3668E-06	2.8777E-10	-2.6831E-14	-2.9742E+04	8.9098E+00
	3.9931E+00	-5.2845E-04	2.6960E-06	-1.4202E-09	2.4155E-13	-3.0273E+04	-2.9219E-03
H_2O_2	3.1980E+00	1.0073E-02	-9.6539E-06	4.9375E-09	-9.9413E-13	-1.7729E+04	7.0820E+00
	2.8691E+00	7.6232E-03	4.8732E-06	-1.7734E-08	1.0258E-11	-1.7577E+04	9.3094E+00
O	2.9946E+00	-9.0737E-04	6.1892E-07	-1.8525E-10	2.0706E-14	2.9048E+04	2.4191E+00
	2.8864E+00	-1.2513E-03	1.5953E-06	-9.0030E-10	1.8673E-13	2.9151E+04	3.2223E+00
O_2	4.9746E+00	-1.8212E-03	1.5866E-06	-5.0780E-10	5.8365E-14	-1.7599E+03	-3.9068E+00
	3.2390E+00	7.3184E-04	1.1088E-06	-1.2178E-09	3.3042E-13	-1.0058E+03	5.9483E+00
HNO	6.0981E+00	-2.5571E-03	3.3893E-06	-1.1625E-09	1.2846E-13	1.0016E+04	-8.6260E+00
	3.5630E+00	9.3470E-04	3.1660E-06	-2.5159E-09	5.9613E-13	1.1145E+04	5.8578E+00
HNO_2-CIS	4.1511E+00	6.9323E-03	-3.6058E-06	8.9760E-10	-8.6903E-14	-1.0859E+04	4.1398E+00
	2.0523E+00	1.4683E-02	-1.3511E-05	6.2574E-09	-1.1398E-12	-1.0472E+04	1.4308E+01
HNO_2-TRA	4.4461E+00	6.3159E-03	-3.1789E-06	7.7039E-10	-7.2925E-14	-1.1098E+04	2.7504E+00
	2.4062E+00	1.3888E-02	-1.2884E-05	6.0314E-09	-1.1077E-12	-1.0726E+04	1.2619E+01
HNO_3	5.7512E+00	9.3375E-03	-5.3562E-06	1.4239E-09	-1.4443E-13	-1.8467E+04	-3.9181E+00
	1.0495E+00	2.4158E-02	-2.2459E-05	1.0040E-08	-1.7495E-12	-1.7313E+04	1.9815E+01
N	2.4984E+00	2.3981E-06	-5.2515E-09	2.7069E-12	-1.7296E-16	5.6108E+04	4.1921E+00
	2.4900E+00	5.7103E-05	-9.2157E-08	5.5643E-11	-1.1381E-14	5.6107E+04	4.2241E+00

Species	a_1^*	a_2^*	a_3^*	a_4^*	a_5^*	a_6^*	a_7^*
NO	4.1809E+00	-4.8912E-04	7.3526E-07	-2.9161E-10	3.7724E-14	9.5240E+03	1.1986E+00
	3.7586E+00	-1.5433E-03	3.9697E-06	-2.6981E-09	6.0031E-13	9.8960E+03	4.2247E+00
NO_2	6.3949E+00	-6.0330E-04	1.1126E-06	-4.5038E-10	6.0868E-14	1.6705E+03	-8.5813E+00
	2.8272E+00	6.5106E-03	-3.6013E-06	5.7804E-10	6.7244E-14	3.0108E+03	1.0977E+01
NO_3	4.0480E+00	9.4921E-03	-6.0071E-06	1.7143E-09	-1.8334E-13	7.0278E+03	4.6989E+00
	4.2661E-01	2.4086E-02	-2.5538E-05	1.2589E-08	-2.3614E-12	7.5588E+03	2.1787E+01
N_2	3.6569E+00	8.4793E-05	4.2901E-07	-2.0919E-10	2.8819E-14	-1.2227E+03	1.9241E+00
	3.7326E+00	-1.7118E-03	3.8204E-06	-2.4253E-09	5.1630E-13	-1.0660E+03	2.1262E+00
N_2O	4.0803E+00	4.3772E-03	-2.3543E-06	6.1897E-10	-6.3419E-14	8.3023E+03	1.7214E+00
	2.6928E+00	8.2811E-03	-6.4623E-06	2.5354E-09	-3.9792E-13	8.6956E+03	8.9015E+00
RuO_2	4.7288E+00	4.2913E-03	-3.4385E-06	1.2654E-09	-1.7233E-13	1.4779E+04	4.0365E+00
	4.9058E-01	2.6467E-02	-4.4538E-05	3.3888E-08	-9.6339E-12	1.5366E+04	2.3178E+01
RuO_3	3.4959E+00	1.5684E-02	-1.5223E-05	6.6833E-09	-1.0896E-12	-1.0858E+04	9.5869E+00
	-9.1842E-01	4.5363E-02	-7.7774E-05	6.0405E-08	-1.7525E-11	-1.0577E+04	2.7878E+01
RuO_4	4.1863E+00	2.1213E-02	-2.0630E-05	9.0570E-09	-1.4766E-12	-2.3938E+04	6.0948E+00
	-1.7966E+00	6.1435E-02	-1.0540E-04	8.1860E-08	-2.3750E-11	-2.3556E+04	3.0886E+01
NH	2.8922E+00	1.0562E-03	-1.8476E-07	-7.5563E-12	5.0738E-15	4.2272E+04	5.1577E+00
	3.7398E+00	-1.3700E-03	2.4074E-06	-1.2334E-09	2.2167E-13	4.2036E+04	7.8713E-01
NH_2	2.9195E+00	3.1180E-03	-8.7606E-07	1.0799E-10	-1.9562E-15	2.1869E+04	5.9880E+00
	4.0611E+00	-1.0589E-03	4.4335E-06	-2.7552E-09	5.5915E-13	2.1654E+04	4.4248E-01

* upper row: temperature range from 1500 to 3000 K, lower row: temperature range from 298.15 to 1500 K

B) Thermodynamic dataset (TD)

a. Recommended values of thermodynamic data of $CsBO_2$(g)

T (K)	$C_p°$ (J/mol/K)	$S°$ (J/mol/K)	$-\{G°-H°(T_r*)\}/T$ (J/mol/K)	$H°-H°(T_r*)$ (J/mol)	$\Delta_f H°$ (J/mol)	$\Delta_f G°$ (J/mol)
298.15	58.919	315.519	315.519	0	-696874	-702636
300	59.025	315.883	315.520	109	-696900	-702671
400	63.943	333.574	317.898	6270	-700372	-703704
500	67.612	348.255	322.542	12856	-701713	-704381
600	70.430	360.842	327.902	19764	-703033	-704791
700	72.629	371.871	333.411	26922	-704354	-704979
800	74.363	381.687	338.843	34275	-705686	-704978
900	75.739	390.528	344.103	41782	-707039	-704808
1000	76.840	398.567	349.154	49413	-775549	-700787
1100	77.728	405.934	353.985	57143	-775937	-693292
1200	78.452	412.729	358.601	64953	-776352	-685761
1300	79.047	419.033	363.010	72829	-776796	-678194
1400	79.541	424.909	367.224	80759	-777271	-670592
1500	79.953	430.412	371.255	88735	-777778	-662954
1600	80.301	435.583	375.116	96748	-778318	-655282
1700	80.597	440.460	378.817	104793	-778895	-647575
1800	80.850	445.075	382.371	112866	-779512	-639832
1900	81.068	449.452	385.788	120962	-780172	-632055
2000	81.257	453.615	389.076	129079	-780882	-624241

*T_r: 298.15 K

b. Recommended values of thermodynamic data of $Cs_2Si_4O_9$(s)

T (K)	$C_p°$ (J/mol/K)	$S°$ (J/mol/K)	$-\{G°-H°(T_r*)\}/T$ (J/mol/K)	$H°-H°(T_r*)$ (J/mol)	$\Delta_f H°$ (J/mol)	$\Delta_f G°$ (J/mol)
298.15	239.000	322.100	322.100	0	-4297600	-4045176
300	240.581	323.583	322.104	444	-4297668	-4043609
400	296.199	401.555	332.357	27679	-4302846	-3957283
500	321.996	470.740	353.277	58732	-4300933	-3871078
600	336.055	530.806	377.976	91698	-4297904	-3785380
700	344.573	583.298	403.639	125761	-4294474	-3700228
800	350.137	629.697	429.053	160515	-4290958	-3615576
900	353.983	671.172	453.692	195732	-4287501	-3531361
1000	356.763	708.620	477.343	231276	-4418435	-3440125

*T_r: 298.15 K

c. Recommended values of thermodynamic data of $CsFeSiO_4$(s)

T (K)	$C_p°$ (J/mol/K)	$S°$ (J/mol/K)	$-\{G°-H°(T_r*)\}/T$ (J/mol/K)	$H°-H°(T_r*)$ (J/mol)	$\Delta_f H°$ (J/mol)	$\Delta_f G°$ (J/mol)
298.15	132.365	177.900	177.900	0	-1657000	-1548580
300	132.755	179.000	178.073	278	-1656722	-1547959
400	148.090	229.359	188.577	16313	-1640703	-1512989
500	157.275	268.020	200.641	33689	-1623341	-1477334
600	163.515	299.754	213.403	51811	-1605234	-1441566
700	167.910	326.803	226.411	70274	-1586786	-1405991
800	170.918	350.403	239.468	88748	-1568328	-1370817
900	172.757	371.315	252.500	106933	-1550160	-1336205
1000	173.545	390.042	265.495	124547	-1532631	-1298581

*T_r: 298.15 K

This is a blank page.

国際単位系（SI）

表１．SI 基本単位

基本量	SI 基本単位	
	名称	記号
長さ	メートル	m
質量	キログラム	kg
時間	秒	s
電流	アンペア	A
熱力学温度	ケルビン	K
物質量	モル	mol
光度	カンデラ	cd

表２．基本単位を用いて表されるSI組立単位の例

組立量	SI 組立単位	
	名称	記号
面積	平方メートル	m^2
体積	立方メートル	m^3
速さ，速度	メートル毎秒	m/s
加速度	メートル毎秒毎秒	m/s^2
波数	毎メートル	m^{-1}
密度，質量密度	キログラム毎立方メートル	kg/m^3
面積密度	キログラム毎平方メートル	kg/m^2
比体積	立方メートル毎キログラム	m^3/kg
電流密度	アンペア毎平方メートル	A/m^2
磁界の強さ	アンペア毎メートル	A/m
量濃度(a)，濃度	モル毎立方メートル	mol/m^3
質量濃度	キログラム毎立方メートル	kg/m^3
輝度	カンデラ毎平方メートル	cd/m^2
屈折率(b)	（数字の） 1	1
比透磁率(b)	（数字の） 1	1

(a) 量濃度（amount concentration）は臨床化学の分野では物質濃度（substance concentration）ともよばれる。
(b) これらは無次元量あるいは次元１をもつ量であるが、そのことを表す単位記号である数字の１は通常は表記しない。

表３．固有の名称と記号で表されるSI組立単位

組立量	SI 組立単位			
	名称	記号	他のSI単位による表し方	SI基本単位による表し方
平面角	ラジアン(b)	rad	1 (b)	m/m
立体角	ステラジアン(b)	sr(c)	1 (b)	m^2/m^2
周波数	ヘルツ(d)	Hz		s^{-1}
力	ニュートン	N		$m\ kg\ s^{-2}$
圧力，応力	パスカル	Pa	N/m^2	$m^{-1}\ kg\ s^{-2}$
エネルギー，仕事，熱量	ジュール	J	N m	$m^2\ kg\ s^{-2}$
仕事率，工率，放射束	ワット	W	J/s	$m^2\ kg\ s^{-3}$
電荷，電気量	クーロン	C		s A
電位差（電圧），起電力	ボルト	V	W/A	$m^2\ kg\ s^{-3}\ A^{-1}$
静電容量	ファラド	F	C/V	$m^{-2}\ kg^{-1}\ s^4\ A^2$
電気抵抗	オーム	Ω	V/A	$m^2\ kg\ s^{-3}\ A^{-2}$
コンダクタンス	ジーメンス	S	A/V	$m^{-2}\ kg^{-1}\ s^3\ A^2$
磁束	ウエーバ	Wb	Vs	$m^2\ kg\ s^{-2}\ A^{-1}$
磁束密度	テスラ	T	Wb/m^2	$kg\ s^{-2}\ A^{-1}$
インダクタンス	ヘンリー	H	Wb/A	$m^2\ kg\ s^{-2}\ A^{-2}$
セルシウス温度	セルシウス度(e)	℃		K
光束	ルーメン	lm	cd sr(c)	cd
照度	ルクス	lx	lm/m^2	m^{-2} cd
放射性核種の放射能(f)	ベクレル(d)	Bq		s^{-1}
吸収線量，比エネルギー分与，カーマ	グレイ	Gy	J/kg	$m^2\ s^{-2}$
線量当量，周辺線量当量，方向性線量当量，個人線量当量	シーベルト(g)	Sv	J/kg	$m^2\ s^{-2}$
酸素活性	カタール	kat		s^{-1} mol

(a)SI接頭語は固有の名称と記号を持つ組立単位と組み合わせても使用できる。しかし接頭語を付した単位はもはやコヒーレントではない。
(b)ラジアンとステラジアンは数字の１に対する単位の特別な名称で、量についての情報をつたえるために使われる。実際には、使用する時には記号radおよびsrが用いられるが、習慣として組立単位としての記号である数字の１は明示されない。
(c)測光学ではステラジアンという名称と記号srを単位の表し方の中に、そのまま維持している。
(d)ヘルツは周期現象についてのみ、ベクレルは放射性核種の統計的過程についてのみ使用される。
(e)セルシウス度はケルビンの特別な名称で、セルシウス温度を表すために使用される。セルシウス度とケルビンの単位の大きさは同一である。したがって、温度差や温度間隔を表す数値はどちらの単位で表しても同じである。
(f)放射性核種の放射能（activity referred to a radionuclide）は、しばしば誤った用語で"radioactivity"と記される。
(g)単位シーベルト（PV,2002,70,205）についてはCIPM勧告2（CI-2002）を参照。

表４．単位の中に固有の名称と記号を含むSI組立単位の例

組立量	SI 組立単位		
	名称	記号	SI 基本単位による表し方
粘度	パスカル秒	Pa s	$m^{-1}\ kg\ s^{-1}$
力のモーメント	ニュートンメートル	N m	$m^2\ kg\ s^{-2}$
表面張力	ニュートン毎メートル	N/m	$kg\ s^{-2}$
角速度	ラジアン毎秒	rad/s	$m\ m^{-1}\ s^{-1}=s^{-1}$
角加速度	ラジアン毎秒毎秒	rad/s^2	$m\ m^{-1}\ s^{-2}=s^{-2}$
熱流密度，放射照度	ワット毎平方メートル	W/m^2	$kg\ s^{-3}$
熱容量，エントロピー	ジュール毎ケルビン	J/K	$m^2\ kg\ s^{-2}\ K^{-1}$
比熱容量，比エントロピー	ジュール毎キログラム毎ケルビン	J/(kg K)	$m^2\ s^{-2}\ K^{-1}$
比エネルギー	ジュール毎キログラム	J/kg	$m^2\ s^{-2}$
熱伝導率	ワット毎メートル毎ケルビン	W/(m K)	$m\ kg\ s^{-3}\ K^{-1}$
体積エネルギー	ジュール毎立方メートル	J/m^3	$m^{-1}\ kg\ s^{-2}$
電界の強さ	ボルト毎メートル	V/m	$m\ kg\ s^{-3}\ A^{-1}$
電荷密度	クーロン毎立方メートル	C/m^3	m^{-3} s A
表面電荷	クーロン毎平方メートル	C/m^2	m^{-2} s A
電束密度，電気変位	クーロン毎平方メートル	C/m^2	m^{-2} s A
誘電率	ファラド毎メートル	F/m	$m^{-3}\ kg^{-1}\ s^4\ A^2$
透磁率	ヘンリー毎メートル	H/m	$m\ kg\ s^{-2}\ A^{-2}$
モルエネルギー	ジュール毎モル	J/mol	$m^2\ kg\ s^{-2}\ mol^{-1}$
モルエントロピー，モル熱容量	ジュール毎モル毎ケルビン	J/(mol K)	$m^2\ kg\ s^{-2}\ K^{-1}\ mol^{-1}$
照射線量（X線及びγ線）	クーロン毎キログラム	C/kg	kg^{-1} s A
吸収線量率	グレイ毎秒	Gy/s	$m^2\ s^{-3}$
放射強度	ワット毎ステラジアン	W/sr	$m^4\ m^{-2}\ kg\ s^{-3}=m^2\ kg\ s^{-3}$
放射輝度	ワット毎平方メートル毎ステラジアン	$W/(m^2\ sr)$	$m^2\ m^{-2}\ kg\ s^{-3}=kg\ s^{-3}$
酵素活性濃度	カタール毎立方メートル	kat/m^3	$m^{-3}\ s^{-1}$ mol

表５．SI 接頭語

乗数	名称	記号	乗数	名称	記号
10^{24}	ヨタ	Y	10^{-1}	デシ	d
10^{21}	ゼタ	Z	10^{-2}	センチ	c
10^{18}	エクサ	E	10^{-3}	ミリ	m
10^{15}	ペタ	P	10^{-6}	マイクロ	μ
10^{12}	テラ	T	10^{-9}	ナノ	n
10^9	ギガ	G	10^{-12}	ピコ	p
10^6	メガ	M	10^{-15}	フェムト	f
10^3	キロ	k	10^{-18}	アト	a
10^2	ヘクト	h	10^{-21}	ゼプト	z
10^1	デカ	da	10^{-24}	ヨクト	y

表６．SIに属さないが、SIと併用される単位

名称	記号	SI 単位による値
分	min	1 min=60 s
時	h	1 h =60 min=3600 s
日	d	1 d=24 h=86 400 s
度	°	1°=(π/180) rad
分	’	1’=(1/60)°=(π/10 800) rad
秒	”	1”=(1/60)’=(π/648 000) rad
ヘクタール	ha	1 ha=1 $hm^2=10^4m^2$
リットル	L, l	1 L=1 l=1 $dm^3=10^3cm^3=10^{-3}m^3$
トン	t	1 t=10^3 kg

表７．SIに属さないが、SIと併用される単位で、SI単位で表される数値が実験的に得られるもの

名称	記号	SI 単位で表される数値
電子ボルト	eV	1 eV=1.602 176 53(14)×10^{-19}J
ダルトン	Da	1 Da=1.660 538 86(28)×10^{-27}kg
統一原子質量単位	u	1 u=1 Da
天文単位	ua	1 ua=1.495 978 706 91(6)×10^{11}m

表８．SIに属さないが、SIと併用されるその他の単位

名称	記号	SI 単位で表される数値
バール	bar	1 bar=0.1MPa=100 kPa=10^5Pa
水銀柱ミリメートル	mmHg	1 mmHg≈133.322Pa
オングストローム	Å	1 Å=0.1nm=100pm=10^{-10}m
海里	M	1 M=1852m
バーン	b	1 b=100fm^2=$(10^{-12}cm)^2$=$10^{-28}m^2$
ノット	kn	1 kn=(1852/3600)m/s
ネーパ	Np	SI単位との数値的な関係は、対数量の定義に依存。
ベル	B	
デシベル	dB	

表９．固有の名称をもつCGS組立単位

名称	記号	SI 単位で表される数値
エルグ	erg	1 erg=10^{-7} J
ダイン	dyn	1 dyn=10^{-5}N
ポアズ	P	1 P=1 dyn s cm^{-2}=0.1Pa s
ストークス	St	1 St =1$cm^2\ s^{-1}$=$10^{-4}m^2\ s^{-1}$
スチルブ	sb	1 sb =1cd cm^{-2}=10^4cd m^{-2}
フォト	ph	1 ph=1cd sr cm^{-2} =10^4lx
ガル	Gal	1 Gal =1cm s^{-2}=$10^{-2}ms^{-2}$
マクスウエル	Mx	1 Mx = 1G cm^2=10^{-8}Wb
ガウス	G	1 G =1Mx cm^{-2} =10^{-4}T
エルステッド(a)	Oe	1 Oe ≙ $(10^3/4\pi)$A m^{-1}

(a) ３元系のCGS単位系とSIでは直接比較できないため、等号「 ≙ 」は対応関係を示すものである。

表10．SIに属さないその他の単位の例

名称	記号	SI 単位で表される数値
キュリー	Ci	1 Ci=3.7×10^{10}Bq
レントゲン	R	1 R = 2.58×10^{-4}C/kg
ラド	rad	1 rad=1cGy=10^{-2}Gy
レム	rem	1 rem=1 cSv=10^{-2}Sv
ガンマ	γ	1 γ=1 nT=10^{-9}T
フェルミ		1 フェルミ=1 fm=10^{-15}m
メートル系カラット		1 メートル系カラット= 0.2 g = 2×10^{-4}kg
トル	Torr	1 Torr = (101 325/760) Pa
標準大気圧	atm	1 atm = 101 325 Pa
カロリー	cal	1 cal=4.1858J（「15℃」カロリー），4.1868J（「IT」カロリー），4.184J（「熱化学」カロリー）
ミクロン	μ	1 μ =1μm=10^{-6}m

（第8版，2006年）